Progress In Electromagnetics Research, PIER 11, 143–198, 1995

COLLOCATION METHOD FOR WAVE PROPAGATION THROUGH OPTICAL WAVEGUIDING STRUCTURES

A. Sharma

1. Introduction

Recently, several methods have been developed to propagate optical beams or total fields through optical waveguiding structures. The advantage of treating total fields, rather than individual modes is manyfold. The analysis is not restricted to uniform or near uniform waveguides and one can handle, in principle, arbitrary index and/or geometry variations along the direction of propagation. Further, one does not have to deal with radiation modes explicitly as these are included in the total field propagating along the waveguiding structure. The most common of these methods is the Beam Propagation Method (BPM) which was first used to propagate laser beams through atmosphere [1]. It was later used for beam propagation through optical fibers [2–6] and through rib waveguides [7]. This method is discussed in detail elsewhere in this volume. Likewise, several other methods, which have lately been developed, are discussed in this volume in other chapters.

In the present chapter, we discuss a method, that we have developed recently for solving the Helmholtz equation. The method is based on the collocation principle and has some unique features in comparison to other methods. The aim in this chapter is to describe the basic principles of this method, its applications to a number of waveguiding problems–both linear and nonlinear, and to compare, through some numerical examples, the computational efficiency and accuracy with those of the BPM.

A waveguide structure is defined by its refractive index distribution $n^2(x, y, z)$ which contains all information regarding interfaces also. The electromagnetic fields that propagate through such a dielectric structure must satisfy the Maxwell equations. However, in a majority of practical waveguiding structures (we will confine our discussion to such cases), the relative variation of the refractive index

is sufficiently small to allow the scalar wave approximation. It, then, suffices to consider instead a much simpler Helmholtz equation:

$$\frac{\partial^2\psi}{\partial x^2}+\frac{\partial^2\psi}{\partial y^2}+\frac{\partial^2\psi}{\partial z^2}+k_0^2n^2(x,y,z)\psi(x,y,z)=0 \tag{1}$$

where $\psi(x,y,z)$ represents one of the cartesian components of the electric field (generally referred to as the scalar field). The time dependence of the field has been assumed to be $\exp(i\omega t)$ and $k_0=\omega/c$.

The problem that is addressed in this chapter is then to obtain the solutions $\psi(x,y,z)$ of Eq. 1 given the field $\psi(x,y,z_0)$ at a plane $z=z_0$. Thus, we are dealing with an initial value problem with respect to the variable z (which is generally taken as the overall direction of propagation). However, the presence of the partial derivatives with respect to the transverse coordinates (x and y) makes this problem much more complex and one has to devise special methods even to obtain numerical solutions. We will discuss, in this chapter, the applications of the collocation method to this problem and its further development that we have made recently [8–17]. For simplicity we shall confine our discussions, initially to 2-dimensional structures and return to 3-D structures later in Sec. 6. Thus, we consider for the present a planar refractive index distribution, $n^2(x,z)$ for which the Helmholtz equation takes the form

$$\frac{\partial^2\psi}{\partial x^2}+\frac{\partial^2\psi}{\partial z^2}+k_0^2n^2(x,z)\psi(x,z)=0 \tag{2}$$

and z is assumed to be the general direction of propagation. In Sec. 2, we have discussed the basic collocation principle and its application to the solution of Eq. 2. Our method uses the orthogonal collocation method and hence, we refer to it as the OCM. In Sec. 3, an unconditionally stable form of the collocation method is developed using the split-step procedure and we shall refer to this method as the split-step collocation method (SSCM). Use of variable transformation makes the collocation method more efficient, as we discuss in Sec. 4. This method then is referred to as the variable transformed collocation method (VTCM). All these methods use the Hermite-Gauss functions as the basis functions. However, the collocation method is open to the choice of basis functions, and in Sec. 5, we discuss the sinusoidal functions based collocation method (SCM). Section 6 is devoted to the discussion on the application of the basic method, the OCM, to

three-dimensional (3-D) propagation. Other forms of the method, the SSCM, the VTCM and the SCM can also be used for 3-D propagation; these are, however, not included in this chapter. Section 7 discusses some applications for which the collocation method has certain distinct advantages and methods like the BPM cannot, in general, be used. Finally, in Sec. 8, we discuss the application of the collocation method for nonlinear pulse propagation through optical fibers.

2. Basic Collocation Method

Collocation methods have been used since the turn of this century for solving integral equations. These were first applied to solution of differential equations by Frazer, Jones and Skan [18] in 1937 and independently by Lanczos [19,20] in 1938. The collocation method belongs to the family of methods used for solving differential equations which can be grouped together under the common name – the method of weighted residuals [21]. In the collocation method, the solution of a differential equation is sought in the form of a linear expansion as a polynomial or over a set of polynomials or functions. The coefficients of expansion are obtained by imposing the condition that the expansion satisfies the differential equation exactly at certain discrete points on the independent variable axis (or plane). These points are referred to as the collocation points. In earlier methods, these points were chosen to be equidistant. However, Lanczos [20] showed that such a choice may lead to divergence in results (a phenomenon termed as 'Runge divergence') and suggested the use of orthogonal polynomials as the basis functions for the expansion. Later, Villadsen and Stewart [22] developed this concept further and called it "orthogonal collocation". Fletcher [23] has shown that the orthogonal collocation gives results with accuracies comparable to the Galerkin method and its implementation is much simpler. Further, the equidistant collocation yields poorer results in comparison to the orthogonal collocation [23]. Orthogonal collocation has been applied using the Radau, Tchebycheff and Legendre polynomials to solve a variety of chemical engineering problems (see, *e.g.*, [24]). In all these problems the range of the independent variables is finite. We have, for the first time, developed [8] the collocation method for the Helmholtz equation which is over an infinite range. We have used the Hermite-Gauss, the Laguerre-

Gauss [25] and the sinusoidal functions as the basis functions. We have used the orthogonal collocation method (OCM) which is outlined in Sec. 2.1.

2.1 Orthogonal Collocation Method (OCM)

We begin with the Helmholtz equation for 2-D propagation, Eq. 2, and seek its solution for $\psi(x, z)$ as a linear combination over a set of suitable orthogonal functions, $\phi_n(x)$:

$$\psi(x, z) = \sum_{n=1}^{N} c_n(z)\phi_n(x) \tag{3}$$

where $c_n(z)$ are the expansion coefficients. The choice of $\phi_n(x)$ depends on the boundary conditions and the symmetry of the guiding structure. For a planar structure, for example, the Hermite-Gauss functions are suitable while for a cylindrical structure the Laguerre-Gauss functions would be more appropriate (see Sec. 5 for further discussion on the choice of basis functions). For the present, we have

$$\phi_n(x) = \mathcal{N}_{n-1} H_{n-1}(\alpha x) \exp(-\frac{1}{2}\alpha^2 x^2) \tag{4}$$

where $\mathcal{N}_{n-1}$ is the normalization constant and α is a parameter which can be chosen arbitrarily, but its choice can influence the accuracy for a given value of N [9]. Obviously, the accuracy of expansion in Eq. 3 improves as N increases. Since Eq. 2 cannot, in general, be solved exactly, an approximate solution is sought by imposing certain conditions which determine the coefficients, $c_n(z)$. In the collocation method, this is done by requiring that the differential equation, Eq. 2, is satisfied *exactly* by the expansion in Eq. 3 at N collocation points $x_j, j = 1, 2, \ldots, N$. This implies that we can uniquely determine only N coefficients in the expansion and thus the orthogonal functions used in the expansion are $\phi_1, \phi_2, \ldots, \phi_N$. In the orthogonal collocation method, the collocation points x_j are chosen such that these are the zeroes of ϕ_{N+1}. Thus,

$$H_N(\alpha x_j) = 0, \quad j = 1, 2, \ldots, N \tag{5}$$

The Hermite polynomial H_N has N distinct zeroes which are well documented in the tables for the Hermite-Gauss quadrature formulae

[25,26]. Writing the Helmholtz equation, Eq. 2 at each of these collocation points, we obtain a set of N total differential equations

$$\left.\frac{\partial^2\psi}{\partial x^2}\right|_{x=x_j} + \frac{d^2\psi_j}{dz^2} + k_0^2 n^2(x_j, z)\psi_j(z) = 0, \quad j = 1, 2, \ldots, N \tag{6}$$

where $\psi_j(z) = \psi(x = x_j, z)$. This set of equations is best handled in the form of a matrix differential equation. Thus, we write

$$\frac{d^2\mathbf{\Psi}}{dz^2} + \mathbf{D} + \mathbf{R}\mathbf{\Psi} = 0 \tag{7}$$

where

$$\mathbf{\Psi}(z) = \text{col.}[\psi(x_1, z) \;\; \psi(x_2, z) \;\; \ldots \;\; \psi(x_N, z)] \tag{8}$$

$$\mathbf{R}(z) = k_0^2 \times \text{diag.}[n^2(x_1, z) \;\; n^2(x_2, z) \;\; \ldots \;\; n^2(x_N, z)] \tag{9}$$

$$\mathbf{D}(z) = \text{col.}\left[\left.\frac{\partial^2\psi}{\partial x^2}\right|_{x=x_1} \;\; \left.\frac{\partial^2\psi}{\partial x^2}\right|_{x=x_2} \;\; \ldots \;\; \left.\frac{\partial^2\psi}{\partial x^2}\right|_{x=x_N}\right] \tag{10}$$

Further, we can write the expansion in Eq. 3 at the collocation points as

$$\psi(x_j, z) = \sum_{n=1}^{N} c_n(z)\phi_n(x_j), \quad j = 1, 2, \ldots, N \tag{11}$$

which can also be written in the matrix form as

$$\Psi(z) = \mathbf{A}\mathbf{C}(z) \tag{12}$$

where

$$\mathbf{C}(z) = \text{col.}\,[c_1(z) \;\; c_2(z) \;\; \ldots \;\; c_N(z)] \tag{13}$$

and

$$\mathbf{A} = \begin{pmatrix} \phi_1(x_1) & \phi_2(x_1) & \ldots & \phi_N(x_1) \\ \phi_1(x_2) & \phi_2(x_2) & \ldots & \phi_N(x_2) \\ \vdots & \vdots & \ddots & \vdots \\ \phi_1(x_N) & \phi_2(x_N) & \ldots & \phi_N(x_N) \end{pmatrix} \tag{14}$$

Similarly, by differentiating Eq. 3 twice with respect to x and writing the resulting equation at each of the collocation points, we obtain

$$\mathbf{D}(z) = \mathbf{B}\mathbf{C}(z) \tag{15}$$

where

$$\mathbf{B} = \begin{pmatrix} \left.\frac{\partial^2\phi_1}{\partial x^2}\right|_{x_1} & \left.\frac{\partial^2\phi_2}{\partial x^2}\right|_{x_1} & \cdots & \left.\frac{\partial^2\phi_N}{\partial x^2}\right|_{x_1} \\ \left.\frac{\partial^2\phi_1}{\partial x^2}\right|_{x_2} & \left.\frac{\partial^2\phi_2}{\partial x^2}\right|_{x_2} & \cdots & \left.\frac{\partial^2\phi_N}{\partial x^2}\right|_{x_2} \\ \vdots & \vdots & \ddots & \vdots \\ \left.\frac{\partial^2\phi_1}{\partial x^2}\right|_{x_N} & \left.\frac{\partial^2\phi_2}{\partial x^2}\right|_{x_N} & \cdots & \left.\frac{\partial^2\phi_N}{\partial x^2}\right|_{x_N} \end{pmatrix} \tag{16}$$

Substituting from Eq. 12, $\mathbf{C} = \mathbf{A}^{-1}\mathbf{\Psi}$ into Eq. 15, we get

$$\mathbf{D}(z) = \mathbf{B}\mathbf{A}^{-1}\mathbf{\Psi}(z) \tag{17}$$

and Eq. 7 then takes the form

$$\frac{d^2\mathbf{\Psi}}{dz^2} + \mathbf{S}\mathbf{\Psi}(z) = 0 \tag{18}$$

where

$$\mathbf{S} = \mathbf{B}\mathbf{A}^{-1} + \mathbf{R}(z) = \mathbf{S}_0 + \mathbf{R}(z) \tag{19}$$

We shall refer to Eq. 18 as the collocation equation. In deriving this equation from the Helmholtz equation, Eq. 2, no approximation has been made except that N is finite and Eq. 18 is exactly equivalent to Eq. 2 as $N \to \infty$. Equation 18 is a matrix total differential equation and can be solved as an initial value problem using any standard method such as the Runge-Kutta method or the predictor-corrector method [25,27].

The field represented by $\mathbf{\Psi}(z)$ varies rapidly on account of its phase factor. In a homogeneous medium, this phase factor can be exactly taken out as $\mathbf{\Psi}(z) = \mathcal{X}\exp(-ikz)$ where k is the wave number in that medium and $\mathcal{X}$ is a constant matrix. In a waveguiding structure, one can similarly write

$$\mathbf{\Psi}(z) = \mathcal{X}(z)e^{-ikz} \tag{20}$$

where $\mathcal{X}(z)$ is a slowly varying envelope of the wave and $k = k_0 n_{ref}$ with n_{ref} being the index of a reference medium (a convenient choice is the cladding or the substrate index). Substituting from Eq. 20 in Eq. 18, we obtain an equation satisfied by the envelope $\mathcal{X}(z)$:

$$\frac{d^2\mathcal{X}}{dz^2} - 2ik\frac{d\mathcal{X}}{dz} + (\mathbf{S} - k^2\mathbf{I})\mathcal{X}(z) = 0 \tag{21}$$

where $\mathbf{I}$ is a unit matrix. For a mode in a uniform waveguide, it is sufficient to consider the parabolic equation which is obtained by neglecting the second derivative term:

$$\frac{d\mathcal{X}}{dz} = (\mathbf{S} - k^2\mathbf{I})\mathcal{X}(z)/2ik, \tag{22}$$

since the propagation constants and the modal fields obtained from Eq. 21 and Eq. 22 are simply related [4]. Even for a non-uniform waveguide, Eq. 22 is an excellent approximation which is equivalent to the Fresnel approximation [2]. This approximation has been extensively used in the study of waveguides and is in fact an essential approximation for the BPM. In our method, on the other hand, it is optional as one could solve either Eq. 21 or Eq. 22. However, we have found that, in practical waveguiding problems, this approximation is extremely good except near the excitation planes where rapidly varying transient fields exist or in cases where reflections are important (see Sec.7.1). In our examples, we have solved Eq. 22, except in Sec.7.1.

It may be pointed out that $\mathbf{S}(z)$ has the z-dependence only through the diagonal matrix $\mathbf{R}(z)$, and $\mathbf{BA}^{-1}$ is constant. Thus, $\mathbf{BA}^{-1}$ has to be computed just once to solve a waveguide design problem in which the refractive index distribution is changed to get a desired effect on propagation. The matrix $\mathbf{A}$ always has an inverse as long as the collocation points are distinct and the basis functions are linearly independent. Further, in case of orthogonal collocation, $\mathbf{A}^{-1}$ can be obtained by simply multiplying its transpose $\mathbf{A}^T$ by a known diagonal matrix (see Appendix A).

2.2 Numerical Example

In this section, we consider an example to show the accuracy and efficiency of the collocation method. We will compare our results with those obtained using the BPM. In order to show the inherent accuracy of the method, we consider the propagation of the fundamental mode through a uniform waveguide. The modal field does not undergo any change except for a phase factor; hence, any change in the amplitude of the modal field would directly reflect the error in the method of propagation. We also choose an index profile for which the modal field and the propagation constant are analytically known. Thus, the numerical computations have been performed for a secant-hyperbolic profile [28]:

$$n^2(x) = n_2^2 + (n_1^2 - n_2^2)\ \mathrm{sech}^2(x/a) \tag{23}$$

with $a=3\,\mu$m, $n_1=1.45$ and $n_2=1.4476$. We assume the free space wavelength of the propagating wave to be $\lambda_0=1.31\,\mu$m so that the V-value [$V=k_0a\sqrt{n_1^2-n_2^2}$] is 1.2. We consider the incidence of the fundamental mode of the waveguide at $z=0$; thus [28],

$$\psi(x, z=0) = \cosh^{-W}(x/a) \tag{24}$$

where

$$W = a\sqrt{\beta^2 - k_0^2 n_2^2} = \frac{1}{2}\sqrt{1+4V^2} \tag{25}$$

As a measure of accuracy we have computed the correlation factor (CF) of the propagating field at $z=100\,\mu$m with the incident field:

$$CF = \frac{\int \psi^*(x, z=0)\ \psi(x, z=100\,\mu\text{m})\ dz}{\sqrt{\left\{\int |\psi(x, z=0)|^2\, dz\right\}\left\{\int |\psi(x, z=100\,\mu\text{m})|^2\, dz\right\}}} \tag{26}$$

The absolute value of the correlation factor should be unity, since only the phase changes as a mode propagates through the waveguide. Thus, any deviations in $|CF|$ from unity is a direct measure of the accuracy of the method used for computing the propagated field. This quantity is plotted in Fig. 1. For comparison, we have also included the results obtained using the BPM with a grid of 128 points in the cross-section between $-50\,\mu$m to $50\,\mu$m. The value of the extrapolation interval is $2.5\,\mu$m for all calculations. Further, to show the computational efficiency of the method, we have also shown the relative computation time. The Runge-Kutta method has been used to solve Eq. 22.

The figure clearly shows that the collocation method is computationally more efficient than the BPM. For example, an accuracy of $\sim 10^{-9}$ is obtained using BPM with 128 points. The same accuracy is obtained using the collocation method with $N=42$ and the computation time is reduced by about 40%. Further, for N-values between 42 and 55, the collocation method gives better accuracy with smaller computation time in comparison to the BPM with 128 points.

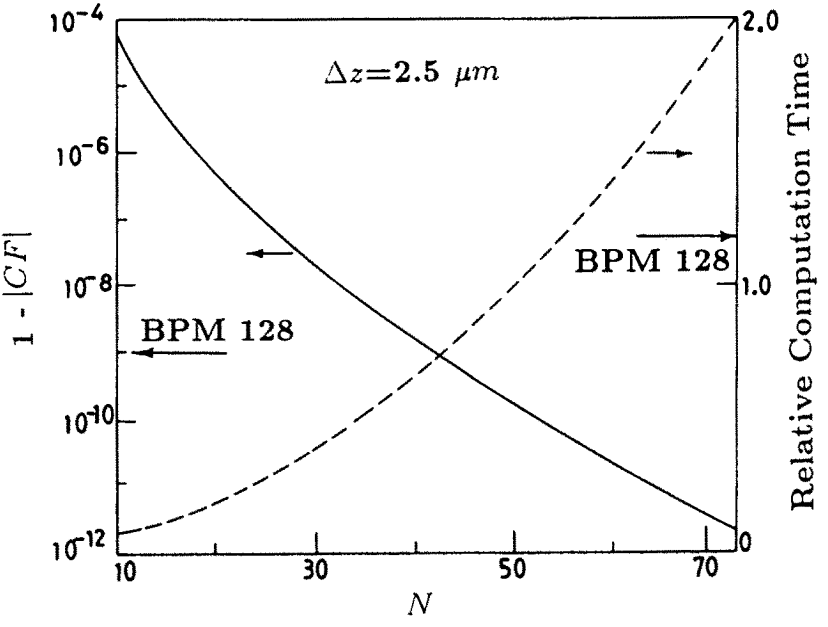

Figure 1. The error in the correlation factor, 1-$|CF|$, as a function of the number of collocation points, N, using the OCM for a uniform waveguide with refractive index distribution defined in Eq. 23. The dashed curve shows the relative computation time. Also indicated are the corresponding quantities for the BPM with 128 sample points.

2.3 Salient Features of the Collocation Method

1. Both the BPM and the collocation method are based on the scalar wave approximation. However, in the formulation of the BPM it is necessary to make a further approximation, namely, the Fresnel approximation, which is justified in most cases of practical interest. However, there are cases where this approximation cannot be used (see, *e.g.*, Sec. 7.1). In the collocation method, the Fresnel approximation is not essential; but, its use reduces the computational effort. No physical or mathematical approximation is made in deriving Eq. 18. The only approximation made is the finiteness

of N. The accuracy improves indefinitely as N increases.

2. It is quite straightforward to obtain propagation constants and modal fields with the collocation method. (see Sec. 7.3) Finding eigenvalues and eigenvectors is much more tedious in the case of the BPM [5]. It is possible to develop a matrix eigenvalue equation using BPM for uniform waveguides using the split-step FFT method [29], but the matrix so obtained is complex with complex eigenvalues whereas in the collocation method, the matrix obtained is real and its eigenvalues are real (see Sec. 7.3).
3. In the collocation method, it is possible to take computational advantage of the special symmetry of the waveguiding structure. For example, in a circularly symmetric fiber or fiber devices, the three dimensional problem can be treated as a two dimensional problem (see Sec. 6.2).
4. The collocation equation, Eq. 18, is equivalent to the Helmholtz equation except for the finiteness of N and this equivalence can be made as accurate as desired by making N large enough. However, computational effort increases at least as N^2 because of the matrices involved. Further, the approximations also come into play due to the numerical method adopted for the solution of the collocation equation. Thus, the results obtained in Fig. 1 using the Runge-Kutta method do not show any saturation in obtainable accuracy as the error is sufficiently small for the Δz-values used due to the single step error in the Runge-Kutta method being of the order of $(\Delta z)^5$. However, other methods (see, *e.g.*, Sec. 3) of lower accuracy do bring in saturation in accuracy.

3. Unconditionally Stable Form of the Collocation Method

3.1 Problem of Stability

The collocation equation obtained in the Sec. 2 can be solved using a variety of numerical methods such as the Runge-Kutta methods or the predictor-corrector methods. These methods can be implemented in various orders, *e.g.*, the most commonly used Runge-Kutta method is of the fourth order and the single step error term is proportional to $(\Delta z)^5$. This generally means that in comparison to a lower order

method, this method gives comparable error with a larger step size, Δz. However, we are dealing with a matrix equation which is basically a set of simultaneous differential equations. In solving such a set of equations, one encounters the problem of stiffness which means that a numerical solution of such a system of equations can become unstable unless the step size, Δz, is very small (see, *e.g.*, [30]). For instance, in the numerical examples of Sec. 2.2, we have used $\Delta z = 2.5\,\mu$m. However, a value of $\Delta z > 5\,\mu$m results in blowing up of the solution after propagation by a few steps. Stiffness is a widely studied problem in applied mathematics (see, *e.g.*, [30,31] for a detailed discussion on this problem). A lower order method (*e.g.*, second order Runge-Kutta method [25]) is more stable than a higher order method. Further, the stiffness gets evened out after a certain number of propagation steps and one could use a larger step size for further propagation. Although there are some special methods available for dealing with stiff systems [30–32], these are somewhat involved to use. To overcome the problem of stiffness, we have developed a different approach to solve the collocation equation. This approach is of the second order and uses the symmetrized splitting of an operator just as in the case of the BPM. It is also necessary, as in the BPM, to use the Fresnel approximation.

3.2 Split-Step Collocation Method (SSCM)

We consider Eq. 22 which can be expressed in the form

$$\frac{d\mathcal{X}}{dz} = [\mathbf{H}_1(z) - \mathbf{H}_2]\mathcal{X}(z)/2ik \tag{27}$$

where $\mathbf{H}_1(z) = \mathbf{R}(z) + \mathbf{D}_1 - k^2\mathbf{I}$ is a z-dependent diagonal matrix and $\mathbf{H}_2 = \mathbf{A}\mathbf{D}_2\mathbf{A}^{-1}$ is a constant square matrix. The matrices $\mathbf{D}_1$ and $\mathbf{D}_2$ are defined as (see Appendix A)

$$\mathbf{D}_1 = \alpha^4 \times \text{diag.}(x_1^2\ x_2^2 \ldots x_N^2) \quad \text{and} \quad \mathbf{D}_2 = \alpha^2 \times \text{diag.}[1\ 3\ 5 \ldots (2N-1)] \tag{28}$$

A formal solution of Eq. 27 can be written as

$$\mathcal{X}(z + \Delta z) = \exp\{[\mathbf{H}_1(z) - \mathbf{H}_2]\Delta z/2ik\}\ \mathcal{X}(z) \tag{29}$$

which, on using the symmetrized splitting, becomes

$$\mathcal{X}(z + \Delta z) = \mathbf{P}\mathbf{Q}(z)\mathbf{P}\mathcal{X}(z) + \bigcirc[(\Delta z)^3] \tag{30}$$

with

$$\mathbf{P} = \exp[-\mathbf{H}_2 \Delta z/4ik]$$

and

$$\mathbf{Q}(z) = \exp[\mathbf{H}_1(z)\Delta z/2ik] \tag{31}$$

The matrix $\mathbf{P}$ is a constant matrix and is to be evaluated only once for a propagation problem. The evaluation of $\mathbf{P}$ can be directly done because of its special form

$$\mathbf{P} = \exp[-\mathbf{A}\mathbf{D}_3\mathbf{A}^{-1}]$$

where the matrix $\mathbf{D}_3 = \mathbf{D}_2\Delta z/4ik$ is a diagonal matrix. Expanding the exponential, we get

$$\mathbf{P} = \mathbf{I} + \sum_{m=1}^{\infty} (\mathbf{A}\mathbf{D}_3\mathbf{A}^{-1})^m/m!$$

and simple manipulations show that

$$(-\mathbf{A}\mathbf{D}_3\mathbf{A}^{-1})^m = (-\mathbf{A}\mathbf{D}_3\mathbf{A}^{-1}).(-\mathbf{A}\mathbf{D}_3\mathbf{A}^{-1}).\ldots.(-\mathbf{A}\mathbf{D}_3\mathbf{A}^{-1})$$

$$= \mathbf{A}(-\mathbf{D}_3)^m\mathbf{A}^{-1}$$

Hence,

$$\mathbf{P} = \mathbf{A}\exp(-\mathbf{D}_3)\mathbf{A}^{-1}$$

The $\exp(-\mathbf{D}_3)$ can be easily evaluated since $\mathbf{D}_2$ is a diagonal matrix and the exponential of a diagonal matrix is a diagonal matrix with the diagonal elements being simply the exponential of the corresponding diagonal elements of the argument matrix.

The matrix $\mathbf{Q}(z)$, on the other hand, can be easily evaluated since the argument of the exponential is a diagonal matrix; thus, $\mathbf{Q}(z)$ is a diagonal matrix whose diagonal elements are the exponentials of the diagonal elements of the argument matrix of $\mathbf{Q}(z)$. Further, since the diagonal matrices commute with each other, we can separate the z-dependent part in $\mathbf{Q}(z)$ as

$$\mathbf{Q}(z) = \mathbf{Q}_1\,\mathbf{Q}_2(z) \tag{32}$$

with

$$\mathbf{Q}_1 = \exp[(\mathbf{D}_1 - p^2\mathbf{I})\Delta z/2ik] \quad \text{and} \quad \mathbf{Q}_2(z) = \exp[\mathbf{R}(z)\Delta z/2ik] \tag{33}$$

The evaluation of $\mathbf{Q}_1$ and $\mathbf{Q}_2(z)$ is simple since these are diagonal matrices.

Thus, a basic propagation step of the split-step collocation method (SSCM) is

$$\mathcal{X}(z + \Delta z) = \mathbf{P}\mathbf{Q}_1\mathbf{Q}_2(z)\mathbf{P}\mathcal{X}(z) + \bigcirc[(\Delta z)^3] \tag{34}$$

which requires two multiplications of a square matrix with a vector and one multiplication of a diagonal matrix with a vector, since $\mathbf{P}\mathbf{Q}_1$ can be evaluated once and treated as a single constant matrix for the propagation. Since all the matrices $\mathbf{P}, \mathbf{Q}_1$ and $\mathbf{Q}_2(z)$ are unitary for real indices, these do not blow up for any value of the arguments. Thus, this algorithm is unconditionally stable for any value of Δz.

However, for obtaining desirable accuracy, the value of Δz is typically only few microns whereas the propagation lengths could be several thousands of microns, indeed even millimeters. Thus, normally propagation over several thousands of steps is to be carried out. In such cases, one does not require to monitor the actual field profile at each step of propagation and in reality several hundred steps are evaluated without visualizing the field. In such cases, the computational effort could be further reduced by making the following transformation

$$\mathcal{Y}(z) = \mathbf{P}\mathcal{X}(z) \tag{35}$$

and

$$\mathbf{\Gamma} = \mathbf{P}^2\mathbf{Q}_1 \tag{36}$$

which is a constant matrix. Equation 34 then takes the form

$$\mathcal{Y}(z + \Delta z) = \mathbf{\Gamma}\mathbf{Q}_2(z)\mathcal{Y}(z) \tag{37}$$

Now, each propagation step requires the multiplication of a diagonal matrix with a column vector and the multiplication of the resulting vector with a square matrix. Conversion from $\mathcal{X}$ to $\mathcal{Y}$ and from $\mathcal{Y}$ to $\mathcal{X}$ is required only at the initial point and the final point, respectively.

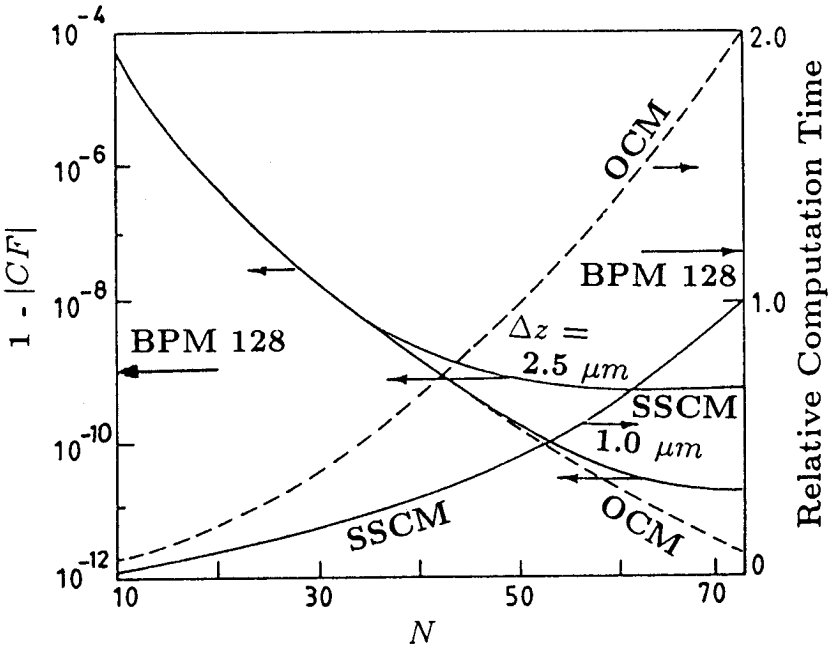

Figure 2. The error in the correlation factor, 1-$|CF|$, and the relative computation time (for $\Delta z = 2.5\,\mu$m) as a function of the number of collocation points, N, using the SSCM for a uniform waveguide with refractive index distribution defined in Eq. 23. The dashed curves correspond to the OCM. Also indicated are the corresponding quantities for the BPM with 128 sample points.

3.3 Examples and Discussion

We again consider the example discussed in Sec. 2.2 and results are given in Fig. 2 where we have plotted the error in the correlation factor as a function of N. The results of Fig. 1 are also included for comparison. The figure shows that the SSCM gives the same accuracy as that obtained by solving the collocation equation in the OCM using the Runge-Kutta method for smaller Δz-values, but the computation time is reduced by a factor of about two. The reduction in the computation time results because, in the SSCM, the number of

multiplications required to propagate the field over one step reduces to $2N(N+1)$ from $4N^2$ in the the Runge-Kutta method. For relatively larger N and Δz, the accuracy curve saturates. This is due to the $(\Delta z)^3$ error in the splitting of the operators (Eq. 30). In the Runge-Kutta method, this error is of the order of $(\Delta z)^5$ [27] and hence, saturation in the correlation error does not appear unless very large N is used; however, one cannot use larger values of Δz, since the Runge-Kutta solution becomes unstable. The SSCM, however, involves only unitary operators (for real refractive indices) and hence, is stable for arbitrary values of Δz. This fact is explicitly shown in Fig. 3 where the error in the correlation factor is plotted as a function of z for different values of Δz. The method remains stable even for $\Delta z = 50\,\mu m$ though the error increases. On the other hand, the error in the OCM with the Runge-Kutta solution blows up for $\Delta z > 5\,\mu m$ after propagation through few steps only.

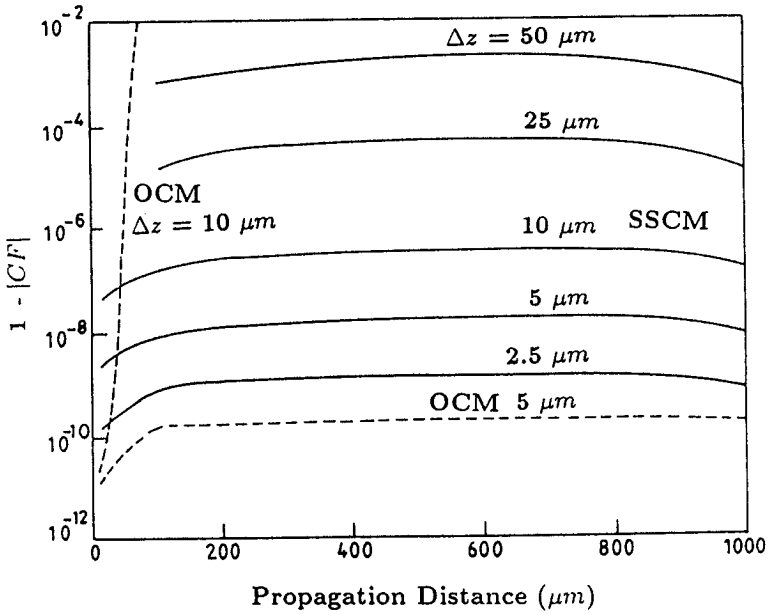

Figure 3. The error in the correlation factor, 1-$|CF|$, as a function of the propagation distance using the SSCM with N=50 for different values of Δz for a uniform waveguide with refractive index distribution defined in Eq. 23. The dashed curves correspond to the OCM (using the Runge-Kutta method).

We consider next, the propagation through a linear taper with index profile given by Eq. 23 with the half-width a now becoming z-dependent as

$$a(z) = a_0 - \zeta z \tag{38}$$

with $a_0 = 3\,\mu$m and $\zeta = 0.1$. We have carried out calculations for a taper of length $10\,\mu$m. Thus, the half width of the guide reduces linearly from $3.0\,\mu$m to $2.0\,\mu$m. The incident field is taken to be the normalized local fundamental mode at $z = 0$. After propagation through the length of the taper, the power lost from the fundamental mode is calculated by taking the difference from unity of the square of the absolute value of the overlap integral between the output field at the end of the taper and the local normalized mode field of the waveguide with half-width $a = a(10\,\mu\text{m})$. The convergence of results is depicted in Fig. 4 where we have plotted the fractional power lost from the fundamental mode as a function of computation time (normalized with respect to the time taken for the BPM with 128 points). The curves are obtained by varying the number of points in both the collocation method and the BPM. The figure shows that the time taken to reach the convergence is about 1/2 in the Runge-Kutta solution (OCM) and about 1/3 with the SSCM in comparison to the BPM. Similar results have been obtained for tapers with cladded parabolic index profile [9].

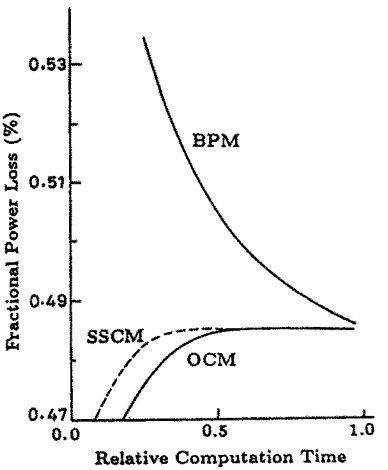

Figure 4. Power lost from the fundamental mode propagating in a taper defined by Eqs.23 & 38 as function of the relative computation time showing the convergence obtained using the OCM, the SSCM and the BPM.

4. Variable Transformed Collocation Method (VTCM)

4.1 Distribution of Sample Points and Accuracy

In the collocation method as well as in the BPM, the propagating field is sampled at certain discrete points along the transverse cross section. The propagation of the field is computed as the variation of the field on these sample points. Obviously, the field is more accurately represented if there is a larger number of sample points; however, then the computational effort also increases. One of the problems that exists with both these methods is that a large fraction of sample points lies outside the guiding region since the sample points are either equally spaced (in the BPM) or nearly equally spaced (in the collocation method). Hence, a very large number of sample points are required to model the field variation accurately in and around the guiding region, and at the same time, to take into account the spread of the field away from this region. It would obviously be more efficient (more accuracy with less computation) if one could redistribute the sample points in such a way that the density of points increases in and around the guiding region, and the transverse extent, covered by the sampled field, also increases. Such a redistribution improves the accuracy of the field propagation method.

A variable transformation, however, converts the Helmholtz equation to such a form that the BPM (based on the Fast Fourier Transform) can no longer be implemented for its solution. On the other hand, such a transformation can be easily incorporated in the collocation method.

4.2 Variable Transformation

We begin with the Helmholtz equation (Eq. 2) for a planar guiding structure and consider the variable transformations

$$x = h(\sigma) \tag{39}$$

$$\psi(x, z) = \sqrt{h'(\sigma)}\, U(\sigma, z) \tag{40}$$

where σ is the new variable, $h(\sigma)$ defines the functional relationship between x and σ (prime denotes differentiation with respect to σ), and $U(\sigma, z)$ is the transformed field. With these transformations,

Eq. 2 becomes

$$\frac{\partial^2 U}{\partial z^2} + f(\sigma)\frac{\partial^2 U}{\partial \sigma^2} + [g(\sigma) + k_0^2 n^2(\sigma, z)]U(\sigma, z) = 0 \tag{41}$$

where

$$f(\sigma) = [h'(\sigma)]^{-2} \tag{42}$$

$$g(\sigma) = \frac{1}{2h'^4}(h''' h' - \frac{3}{2}h'^2) \tag{43}$$

Equation 41 is similar to Eq. 2 in form except that the coefficient of the second term is now variable. It is for this very term that the BPM based on FFT cannot be implemented to solve the equation because the solutions for the corresponding equation with n^2 constant are no longer sinusoidal functions or plane waves. However, the collocation method is general enough to be applicable to this equation also. Thus, using the method described in Sec. 2.1, we can convert Eq. 41 into a matrix equation

$$\frac{d^2\mathbf{U}}{dz^2} + \hat{\mathbf{S}}\mathbf{U}(z) = 0 \tag{44}$$

The vector $\mathbf{U}(z)$ denotes the values of the transformed field at the collocation points as a function of z. The matrix $\hat{\mathbf{S}}$ is defined as

$$\hat{\mathbf{S}} = \mathbf{F}\mathbf{B}\mathbf{A}^{-1} + \mathbf{R}(z) + \mathbf{G} \tag{45}$$

where $\mathbf{R}, \mathbf{F}$ and $\mathbf{G}$ are diagonal matrices with their successive diagonal elements being the values of $k_0^2 n^2(\sigma, z)$, $f(\sigma)$ and $g(\sigma)$, respectively, at the collocation points, which are now defined as the zeroes of $H_N(\alpha\sigma)$. The matrices $\mathbf{A}$ and $\mathbf{B}$ are defined in the same way as in Eqs. 14 & 16 except that now the independent variable is σ and the collocation points are defined above. Once again, we can take out the rapid variations on account of the phase factor; thus, writing $\mathbf{U}(z) = \hat{\mathcal{X}}(z)\exp(-ikz)$, where the envelope of the field $\hat{\mathcal{X}}(z)$ satisfies the following differential equation under the Fresnel approximation

$$\begin{aligned}\frac{d\hat{\mathcal{X}}}{dz} &= (\hat{\mathbf{S}} - k^2\mathbf{I})\hat{\mathcal{X}}(z)/2ik \\ &= (\hat{\mathbf{H}}_1 - \hat{\mathbf{H}}_2)\hat{\mathcal{X}}(z)/2ik\end{aligned} \tag{46}$$

where

$$\hat{\mathbf{H}}_1 = \mathbf{F}\hat{\mathbf{D}}_1 + \mathbf{R}(z) + \mathbf{G} - k^2\mathbf{I} \tag{47}$$

$$\hat{\mathbf{H}}_2 = \mathbf{F}\mathbf{A}\hat{\mathbf{D}}_2\mathbf{A}^{-1} \tag{48}$$

and $\hat{\mathbf{D}}_1$ and $\hat{\mathbf{D}}_2$ are defined as $\mathbf{D}_1$ and $\mathbf{D}_2$ of Eq. 28 for σ_j's. A formal solution of Eq. 46 can then be written as

$$\hat{\mathcal{X}}(z + \Delta z) = \hat{\mathbf{P}}\hat{\mathbf{Q}}(z)\hat{\mathbf{P}}\hat{\mathcal{X}}(z) + \bigcirc[(\Delta z)^3] \tag{49}$$

where symmetric splitting of the operator has been used and

$$\hat{\mathbf{P}} = \exp(-\hat{\mathbf{H}}_2\Delta z/4ik),$$

$$\hat{\mathbf{Q}}(z) = \exp[-\hat{\mathbf{H}}_1(z)\Delta z/2ik].$$

The evaluation of $\hat{\mathbf{Q}}(z)$ is simple as $\hat{\mathbf{H}}_1$ is a diagonal matrix. The evaluation of $\hat{\mathbf{P}}$ now requires the diagonalization of matrix $\hat{\mathbf{H}}_2$; thus, we obtain its eigenvalues, $\mathbf{\Lambda}$, and the eigenvectors, $\mathbf{V}$, so that $\hat{\mathbf{H}}_2 = \mathbf{V}\mathbf{\Lambda}\mathbf{V}^{-1}$ and hence, $\hat{\mathbf{P}} = \mathbf{V}\exp(-\mathbf{\Lambda}\Delta z/2ik)\mathbf{V}^{-1}$ (see Sec.3.2 for details). The evaluation of $\hat{\mathbf{P}}$ is required only once before the actual propagation begins, and the computation involved in each propagation step remains exactly the same as in the SSCM of Sec.3. The matrix $\hat{\mathbf{H}}_2$ is not a symmetric matrix, but is similar to a real symmetric matrix (see Appendix B) and hence, the eigenvalues and the eigenvectors can be easily obtained.

4.3 Choice of Transformation and Examples

The choice of the transformation, $h(\sigma)$, depends on the manner in which the sample points are desired to be distributed. In most cases of guided wave propagation (particularly, in single moded structures), a large fraction of power is confined in the guiding region. Beyond this region, the field decays generally monotonically and slowly extending to a large transverse cross section. For such cases, if the sample points can be crowded in the guiding region and made to cover a larger extent of the transverse cross-section away from the guiding region, the accuracy will definitely improve irrespective of the index profile and the field distribution. The extent of improvement may differ in different cases. There may be other cases too; for example, one may wish to crowd

points in the area where the refractive index is varying relatively more rapidly.

There are, however, certain general conditions that the transformation, $h(\sigma)$, must satisfy. It must be single valued and antisymmetric [$h(-\sigma) = -h(\sigma)$], so that there is a unique one-to-one correspondence between x and σ for both positive and negative values. Further, $h'(\sigma), h''(\sigma)$, and $h'''(\sigma)$ should be continuous functions of σ and $h'(\sigma) \neq 0$. Thus, the simplest form of transformation is $\sigma(1 + \gamma\sigma^2)$. The value of the width constant α would be different for different transformations. The values of α [used in the argument of $H_n(\alpha\sigma)$] and γ are obtained by minimizing the propagation error in a trial propagation through a uniform waveguide over a small length.

Numerical examples using the transformations $h(\sigma) = \sigma(1+\gamma\sigma^2)$ and $h(\sigma) = \sigma(1+\gamma\sigma^4)$ for a sech^2 waveguide of Sec. 2.2 are discussed in [12]. We include here results for the transformation $h(\sigma) = \sinh\sigma$ for the same waveguide. Figure 5 shows the distribution of sample points for $N = 20$ with and without this transformation. The figure shows that without the transformation, the points are nearly evenly distributed in the region upto about $7a$, whereas with the transformation, these points are more crowded upto about $2a$, and the last points in stretched beyond $22a$. Thus, in the transformed method(VTCM), the field values down to about 10^{-9} are "seen" by the method, while in the untransformed case (OCM), fields only down to about 10^{-4} are taken into account. This redistribution has a dramatic effect on the accuracy of propagation as can be seen from Fig. 6 where we have plotted the error in the correlation factor as a function of the number of collocation points N for different values of Δz. There are two distinct features to be noted. Firstly, for smaller values of N ($N < 30$, in the given example), there is an improvement in the accuracy by about three orders of magnitude for all values of Δz. Secondly, the saturation value of accuracy has changed markedly for all values of Δz. Thus, whereas for moderate values of Δz the accuracy worsens, for smaller values of Δz the accuracy improves by several orders of magnitude. For example, an accuracy of 10^{-12} is not achievable even with $N > 60$ and small Δz values in the OCM, this is possible, even with $N < 30$ and $\Delta z \sim 0.2\,\mu$m in the VTCM. Thus, with the help of an appropriate transformation, a better accuracy can be achieved with smaller matrix sizes. This would result in reduction of computational effort.

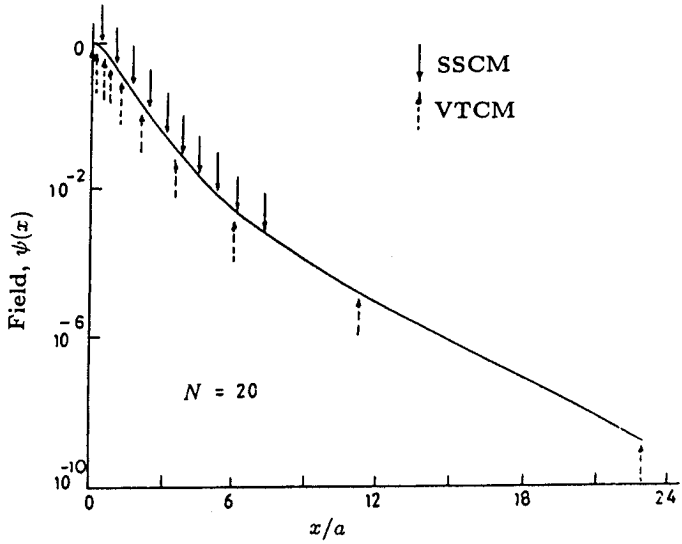

Figure 5. The field, $\psi(x)$, as function of x/a showing the location of the collocation points with (VTCM) and without (SSCM) the transformation $h(\sigma) = \sinh(\sigma)$.

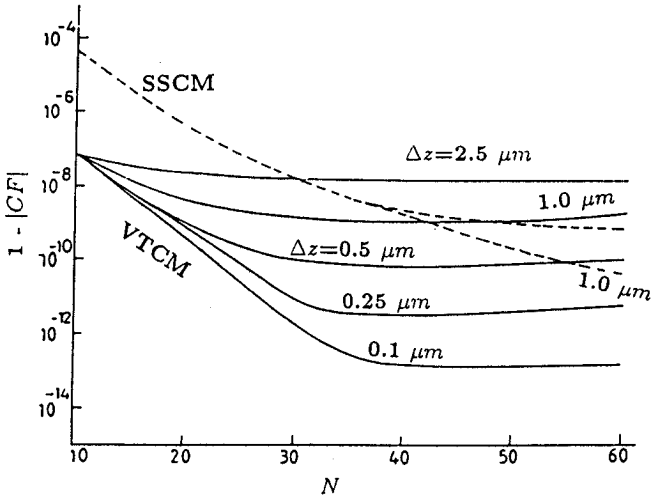

Figure 6. The error in the correlation factor, 1-$|CF|$, as a function of the number of collocation points, N, using the VTCM with $h(\sigma) = \sinh(\sigma)$ and $\alpha = 1.1\,\mu\text{m}^{-1}$ for different values of Δz for a uniform waveguide with refractive index distribution defined in Eq. 23. The dashed curves correspond to the SSCM.

5. Choice of Basis Functions

As discussed in Sec. 2.1, the collocation method is open to the choice of the basis functions, although, for planar waveguiding structures, we have chosen these functions to be the Hermite-Gauss functions. There are, however, certain general conditions that the basis functions should satisfy. First of all, these must satisfy the boundary conditions in the transverse direction. Each function and its derivative must be continuous, since their combination represents the electric field. Further, the function and its derivative should vanish as $x \rightarrow \pm\infty$. The Hermite-Gauss functions satisfy these conditions. The choice of basis functions also depends on the symmetry of the waveguide geometry. For example, for a circularly symmetric index distribution (like in optical fibers), the Laguerre-Gauss functions are better suited (see Sec. 6.2).

The condition of vanishing field and its derivative at $x \rightarrow \pm\infty$ is often simulated at $x = L$, where L is chosen, by trial, to be large enough so that the actual field is negligibly small at this boundary and the accuracy of propagation is least affected by its presence. This does lead to problem of spurious reflection from this boundary and there have been some ways of suppressing this problem. This type of boundary condition is used in the BPM and, in fact, in most methods based on finite element and finite difference algorithms (see, *e.g.*,[33,34]). In the BPM, the electric field is expressed in terms of plane waves, which can be expressed in terms of sinusoidal functions. In this section, we use this type of basis functions in the collocation method. Thus, the new method can be considered as the collocation formulation of the BPM. We shall refer to this method as the sinusoidal function based collocation method (SCM). We have used the split-step form of the collocation method for implementation of the SCM. Thus, like the BPM, it is also based on the Fresnel approximation. The main difference, then, between the SCM and the BPM is the algorithm to propagate the field over the step length of Δz; in the BPM, this is done using the plane wave decomposition and propagating each plane wave, while, in the SCM, the resulting operators are evaluated using matrix algebra. The results obtained using these two methods would, therefore, provide a direct comparison between these two propagation schemes. On the other hand, the only difference between the SCM and the SSCM is the choice of the set of basis functions and, hence, the results obtained

using these two methods would provide a direct comparison between these two sets of basis functions.

5.1 The SCM: Collocation Formulation of the BPM

The sinusoidal functions are the solutions of the Helmholtz equation for a homogeneous medium. However, these functions continue oscillating even as $x \to \pm\infty$. In order to satisfy the condition of vanishing field at large distances, we assume, like in the BPM artificial boundary at $x = \pm L$ where the field is assumed to vanish. With these boundary conditions on a *homogeneous* medium, the Helmholtz equation gives the following solutions:

$$\begin{aligned} \chi_n(x) &= \cos(\nu_n x) \qquad \text{for } n = 1,3,5,\ldots,N-1 \\ &= \sin(\nu_n x) \qquad \text{for } n = 2,4,6,\ldots,N \end{aligned} \tag{50}$$

These functions form an orthogonal set of functions. The boundary condition $\chi_n(x) = 0$ gives $\nu_n = n\pi/2L$. Choosing N to be an even number, we define the collocation points x_j as the zeroes of $\cos(\nu_{N+1}x)$. Thus, the collocation points are

$$x_j = \left(\frac{2j}{N+1} - 1\right)L \qquad j = 1,2,\ldots,N \tag{51}$$

Following the procedure similar to the one described in Sec.2.1, we obtain the following matrix differential equation

$$\frac{d^2\Psi}{dz^2} + \tilde{\mathbf{S}}\Psi(z) = 0 \tag{52}$$

where $\tilde{\mathbf{S}} = \tilde{\mathbf{B}}\tilde{\mathbf{A}}^{-1} + \mathbf{R}(z)$. Further, $\tilde{\mathbf{A}}$ and $\tilde{\mathbf{B}}$ are square matrices with their elements defined as

$$\tilde{A}_{jn} = \chi_n(x_j) \quad \text{and} \quad \tilde{B}_{jn} = \left.\frac{d^2\chi_n}{dx^2}\right|_{x=x_j}; \qquad j = 1,2,\ldots,N \tag{53}$$

and it can be shown that

$$\tilde{\mathbf{B}} = \tilde{\mathbf{A}}\tilde{\mathbf{H}} \tag{54}$$

where

$$\tilde{\mathbf{H}} = \text{diag.}[-\nu_1^2, -\nu_2^2, \ldots, -\nu_N^2] \tag{55}$$

Thus, with $\tilde{\mathbf{S}} = \tilde{\mathbf{A}}\tilde{\mathbf{H}}\tilde{\mathbf{A}}^{-1} + \mathbf{R}(z)$ and the Fresnel approximation, Eq. (52) can be written as

$$\frac{d\tilde{\mathcal{X}}}{dz} = [\tilde{\mathbf{A}}\tilde{\mathbf{H}}\tilde{\mathbf{A}}^{-1} + \mathbf{R}(z) - k^2\mathbf{I}]\tilde{\mathcal{X}}(z)/2ik \tag{56}$$

where $\tilde{\mathcal{X}}(z) = \Psi(z)\exp(ikz)$. Using the symmetrized splitting of operators and a procedure similar to the one used in Sec. 3.2, we can write the formal solution of Eq. (56) to obtain the basic step of the SCM as

$$\tilde{\mathcal{X}}(z + \Delta z) = \tilde{\mathbf{P}}\tilde{\mathbf{Q}}(z)\tilde{\mathbf{P}}\tilde{\mathcal{X}}(z) + \bigcirc[(\Delta z)^3] \tag{57}$$

where

$$\begin{aligned}\tilde{\mathbf{P}} &= \tilde{\mathbf{A}}\ \exp[\tilde{\mathbf{H}}\Delta z/4ik]\ \tilde{\mathbf{A}}^{-1} \\ \tilde{\mathbf{Q}} &= \exp[\mathbf{R}(z)\Delta z/2ik]\ \exp[-k^2\mathbf{I}\Delta z/2ik]\end{aligned} \tag{58}$$

The evaluation of the exponentials in the above expressions can be done analytically since the arguments are diagonal matrices. Equation (57) is exactly same in form as the basic propagation step in the BPM and the basis functions are fairly close to those used in BPM. Therefore, we have justifiably termed this method as the collocation formulation of BPM.

It may be pointed out here that in the SCM, it is possible to take advantage of the variable transformation as discussed in Sec. 4, while in the conventional BPM it is not possible. A detailed discussion on this including numerical examples is given in [14].

5.2 Numerical Examples and Comparisons

In this section, we compare the three methods – the BPM, the SSCM and the SCM, and we again consider the example of Sec. 2.2. The error in the correlation factor is plotted in Fig. 7 for the SSCM, the SCM and the BPM. The value of Δz is 2.5 μm. The figure shows that the SCM is, in general, about an order of magnitude more accurate than the BPM. Thus, the method of solution of the propagation equation in the collocation method is better than in the BPM. The difference in the accuracies obtained using the SSCM and the SCM is much larger showing that the Hermite-Gauss functions are far better

suited than the sinusoidal functions for modeling guided wave propagation. One possible reason could be that the Hermite-Gauss functions are more confined and resemble the waveguide modes more closely than the sinusoidal functions. However, the sinusoidal circular functions are better suited for propagation through the homogeneous media in which the field is not confined to a small region of space.

Another important feature of these methods, apparent from Fig. 7 is that, for sufficiently large value of N, the error saturates. It may be mentioned here that this saturation is mainly due to the method used for solving the matrix differential equation. For example, this saturation value of error is too low to appear on the curves obtained using the Runge-Kutta method [in which the truncation error is $\sim (\Delta z)^5$] for $\Delta z = 2.5\,\mu$m (see Fig. 1), while in the SSCM, it appears (see Fig. 2) at different error levels for different values of Δz (the truncation error is $\sim (\Delta z)^3$). However, in the methods being discussed in this section, there are additional approximations – Fresnel approximation and artificial boundary at a large but finite distance (for the BPM and the SCM). Thus, for relatively larger Δz (typically $\Delta z \geq 1\,\mu$m in our example), the error due to $(\Delta z)^3$-term dominates. This is apparent from Fig. 8 in which all the three methods expectedly show similar qualitative behavior for $\Delta z \geq 1\,\mu$m. For smaller Δz values, this error becomes small and errors due to other approximations (Fresnel, finite window, etc.) become important. These errors are difficult to quantify and a more detailed study involving a larger number of examples would be required. However, our test example on sech^2 waveguide shows (in Fig. 8) that the saturation error in the SSCM continues to decrease, though comparatively slowly, whereas for the SCM it saturates for $\Delta z \geq 1\,\mu$m. The BPM shows a peculiar behavior as the saturation error again increases for $\Delta z \leq 0.5\,\mu$m. Since all other features of the BPM and the SCM are essentially same, this behavior could only be attributed to the FFT-based propagation scheme, or to the fact that the basis functions in BPM do not actually go to zero at the edge of the computational window (we have not used any absorber at the edge of the window).

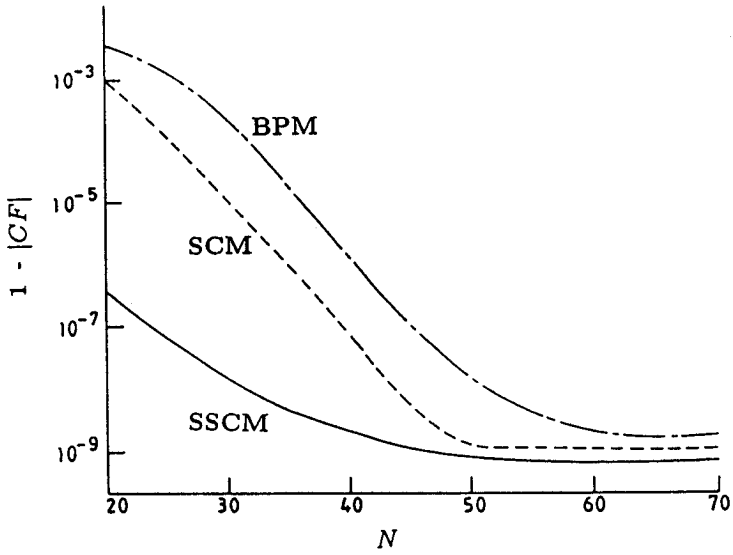

Figure 7. The error in the correlation factor, 1-$|CF|$, as a function of the number of collocation points, N, using the SSCM, the SCM and the BPM for a uniform waveguide with refractive index distribution defined in Eq. 23.

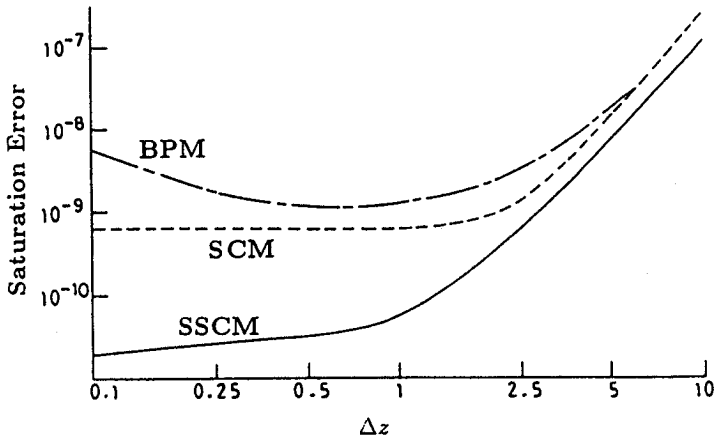

Figure 8. Saturation error as a function of the extrapolation interval, Δz, for the SSCM, the SCM and the BPM.

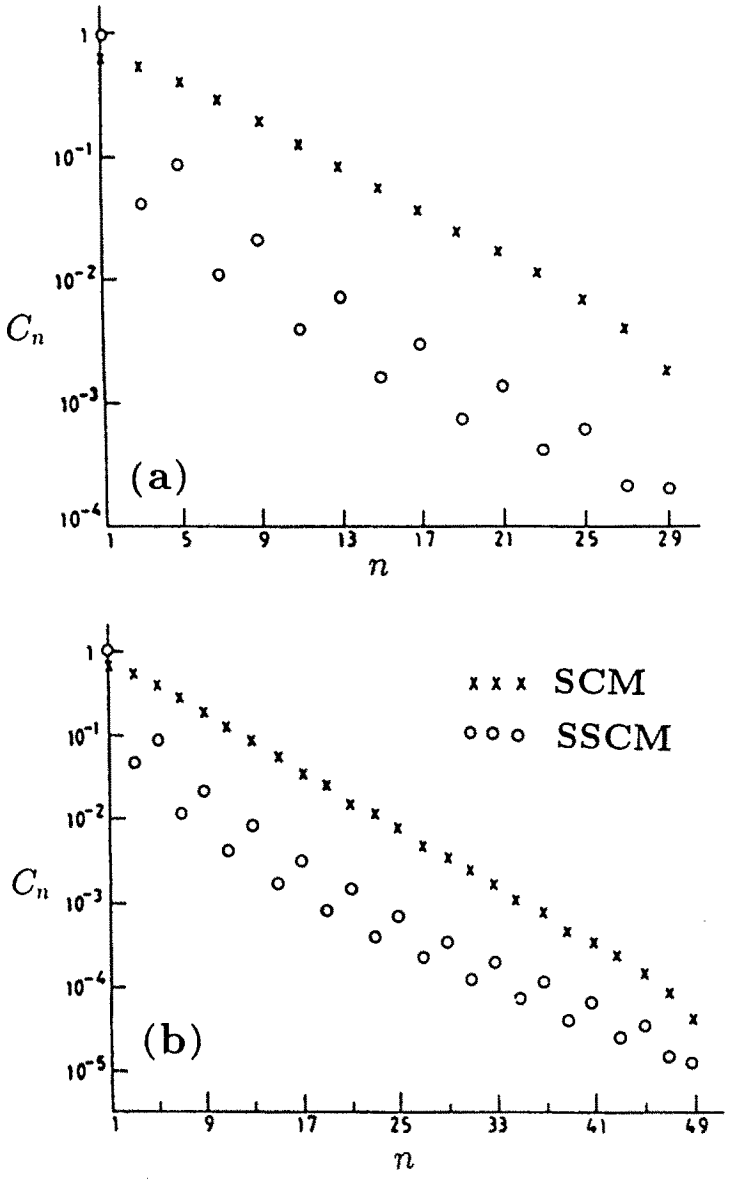

Figure 9. The values of the expansion coefficients, C_n, for different orders, n, of the basis functions used in the SSCM and the SCM for (a) N=30 and (b) N=50.

From the above discussion, it is clear that for guided wave propagation the Hermite-Gauss functions are better suited for the expansion of the guided wave fields. In principle, any such expansions should have infinite terms, and, then the expansion coefficients of the terms of higher order would successively becomes smaller and smaller. By making N finite, we essentially truncate this infinite succession of coefficients, and the coefficients beyond N are effectively made zero. Thus, between $n = N$ and $n = N + 1$, there is effectively a sharp step change in the values of the coefficients. The smaller the value of this step the better is the accuracy of the finite expansion. In Fig. 9a, we give the distribution of the expansion coefficients for the SSCM and the SCM for $N = 30$. Only alternate coefficients are non-zero since the field is symmetric. The figure clearly shows that the last coefficient for the SSCM is $\approx 10^{-4}$, while for the SCM it is $\approx 10^{-3}$. This is one of the main reasons for the difference of 3-orders of magnitude in the propagation accuracy (as shown in Fig. 7). Further confirmation of this aspect is provided from Fig. 9b, where we have shown the values of coefficients for $N = 50$. Now, values of the last coefficients in the SSCM and the SCM are 1.23×10^{-5} and 4.22×10^{-5}, respectively. In both cases, the values of the coefficients have reduced as compared to the values in $N = 30$ and hence, the accuracy of propagation increased (see Fig. 7). Further, the difference in the values of the last coefficients in the SSCM and the SCM values has also become much smaller resulting in smaller difference in the accuracies obtained from the methods for $N = 50$ (see Fig. 7).

6. Application to 3-Dimensional Propagation

In the sections above, we have confined our discussion to two-dimensional guiding structures. In this section, we discuss the extension of the collocation method for 3-D guiding structures. A direct 3-D analysis is much more involved and time consuming and, therefore, in a number of cases modeling is done by reducing the 3-D structure to an equivalent 2-D structure using methods like the effective index method [35,36] or the variational method [37,38], and studying the propagation through the 2-D structure [39]. In such cases, the methods discussed above are useful. However, a 2-D model may at times give erroneous results (See [40]). Thus it becomes necessary to have a general method

to study three dimensional structures.

The collocation method can be easily extended to three dimensions, but, as in the case of the BPM, there is a substantial increase in the computational effort, which may be greater by one or two orders of magnitude in comparison to that in 2-D cases. In general, one has to use cartesian coordinates for 3-D problems, except when the device is made from optical fibers and retains its circular symmetry (as, for example, in fiber tapers). In the latter case, one could use the circular cylindrical coordinates with substantial computational advantage (see Sec. 6.2).

6.1 3-D Structures in Cartesian Coordinates

We now consider the 3-D Helmholtz equation, Eq. 1, and use a double linear expansion of the field in terms of two sets of the Hermite-Gauss functions:

$$\psi(x,y,z) = \sum_{n=1}^{N}\sum_{m=1}^{M} \mathcal{K}_{nm}(z)\ \phi_n(x)\ \eta_m(y) \tag{59}$$

where $\phi_n(x)$ are defined in Eq. 4 and $\eta_m(y)$ are defined in an identical way with y and κ instead of x and α. Following the procedure described in Sec. 2.1, one can define the collocation points on x and y axes and convert Eq. 1 into the following matrix differential equation (see [9] details)

$$\frac{d^2\mathbf{\Psi}}{dz^2} + \mathbf{S_0}\mathbf{\Psi} + \mathbf{\Psi}\mathbf{T}^T + \mathbf{R}(\mathbf{\Psi}) = 0 \tag{60}$$

where $\mathbf{\Psi}$ is now a $N \times M$ matrix defining the field $\psi(x,y)$ at a matrix of collocation points, $\mathbf{S_0}$ is defined in Eq. 19 and $\mathbf{T}$ is defined in an identical way with $\eta_m(y)$ replacing $\phi_n(x)$. $\mathbf{T}^T$ represents the transpose of $\mathbf{T}$. Further, $\mathbf{R}(\mathbf{\Psi})$ is an $N \times M$ matrix with its elements defined as

$$[\mathbf{R}(\mathbf{\Psi})]_{nm} = k_0^2 n^2(x_n, y_m, z)\psi(x_n, y_m, z) \tag{61}$$

Under the Fresnel approximation, we can reduce Eq. 60 to a first order differential equation

$$\frac{d\mathcal{X}}{dz} = [\mathbf{S}\mathcal{X} + \mathcal{X}\mathbf{T}^T + \mathbf{R}(\mathcal{X}) - k^2\mathcal{X}]/2ik \tag{62}$$

where $\mathcal{X}$ and k are defined in Eq. 20. To give an estimate of the increase in computational effort while going over from 2 to 3 dimensions, we have shown, in Table I, the number of multiplications to be performed in each propagation step for both the BPM and the collocation method(OCM). As can be seen from Table I, the increase in the number of multiplications while going over from 2 to 3 dimensions is two times the number of sample points in the transverse cross-section for both the cases. Thus, the increase in the computational effort can be expected to be less in the collocation method, since, as we have seen in Sec. 2.2, the number of collocation points needed to achieve a certain degree of accuracy is substantially less than the number of points needed in the BPM. A numerical example is included in Sec. 6.3.

6.2 3-D Structures in Circular-Cylindrical Coordinates

Optical fibers and fiber based devices fall in this category of guiding structures. If the device is made in such a way that the structure retains its circular symmetry, as in the case of fiber tapers and expanders, then it is more advantageous to work in the circular-cylindrical coordinate system. Further, if one considers field patterns of one kind of azimuthal symmetry at a time, it is possible to write the scalar Helmholtz equation as:

$$\frac{\partial^2\psi}{\partial z^2} + \frac{\partial^2\psi}{\partial r^2} + \frac{1}{r}\frac{\partial\psi}{\partial r} - \frac{l^2}{r^2}\psi + k_0^2 n^2(r,z)\psi(r,z) = 0 \qquad (63)$$

where l is the azimuthal symmetry parameter of the field. The above equation is a partial differential equation and using the collocation method it can be converted into a matrix differential equation. As an illustration, we consider the case of circularly symmetric modes, $l = 0$, and we can expand ψ in terms of the Laguerre-Gauss functions [25] which form a complete set of circularly symmetric functions in the domain $0 \leq r \leq \infty$, and go to zero as $r \to \infty$. Thus, we write

$$\psi(r,z) = \sum_{n=1}^{N} \mathcal{K}_n(z)\ \Theta_n(r) \qquad (64)$$

where

$$\Theta_n(r) = L_{n-1}(b^2r^2)\exp(-\frac{1}{2}b^2r^2) \qquad (65)$$

The corresponding matrix differential equation is

$$\frac{d^2\Psi}{dz^2} + \bar{\mathbf{B}}\bar{\mathbf{A}}^{-1}\Psi + \mathbf{R}(z)\Psi(z) = 0 \tag{66}$$

where the elements of $\bar{\mathbf{A}}, \bar{\mathbf{B}}$ and $\mathbf{R}$ are defined as

$$\begin{aligned} \bar{A}_{jn} &= \Theta_n(r_j), \\ \bar{B}_{jn} &= \frac{d^2\Theta_n}{dr^2} + \frac{1}{r}\frac{d\Theta_n}{dr}\bigg|_{r=r_j}, \\ R_{jn} &= k_0^2 n^2(r_j, z)\delta_{jn} \end{aligned} \tag{67}$$

r_j's denote the collocation points defined as the zeroes of $\Theta_{N+1}(r)$. Under the Fresnel approximation, we then have (*cf.* Eq. 22)

$$\frac{d\mathcal{X}}{dz} = [\bar{\mathbf{B}}\bar{\mathbf{A}}^{-1} + \mathbf{R}(z) - k^2\mathbf{I}]\mathcal{X}(z)/2ik \tag{68}$$

Thus, the computational effort involved in solving Eq. 68 would be of the same order as that in case of planar waveguides.

6.3 Numerical Example

We now consider an example to show the effectiveness of the collocation method for 3-D propagation. We have performed calculations for a circularly symmetric waveguide with a Gaussian profile. We have chosen a circularly symmetric refractive index profile so that we can compare the results obtained using the methods developed in Sec. 6.1 and Sec. 6.2. The refractive index profile is given by

$$n^2(x, y) = n_2^2 + (n_1^2 - n_2^2)\exp[-(x^2 + y^2)/a^2] \tag{69}$$

with $n_1 = 1.45$, $n_2 = 1.435$, $\lambda = 1.3\,\mu$m and $a = 2.5\,\mu$m. We again consider the propagation of the fundamental mode and after a propagation through a distance of $z = 10\,\mu$m, we obtain the error in the correlation factor (defined in an analogous way as in Eq. 26) between the field at $z = 0$ and the field at $z = 10\,\mu$m. This error is plotted, in Fig. 10, as a function of N, (we have taken $M = N$). The continuous curve is obtained using the method of Sec. 6.1, while the dash-dot curve is

obtained using the method of Sec. 6.2. The order of accuracy obtained is nearly the same for a given N in the two cases; however, in the case of circularly symmetric basis functions, the computational effort is much less (about 1/40 for $N=30$). The figure also shows that the accuracy of about 10^{-9}, obtained using the 3D-BPM with 60 points, can be achieved by using 30 collocation points (the method of Sec. 6.1) and the time taken is about one third (the dashed curve shows relative computation time for method of Sec. 6.1). Thus, we see that even in the case of three dimensional waveguides our method works better than the BPM, as can be expected from Table 1.

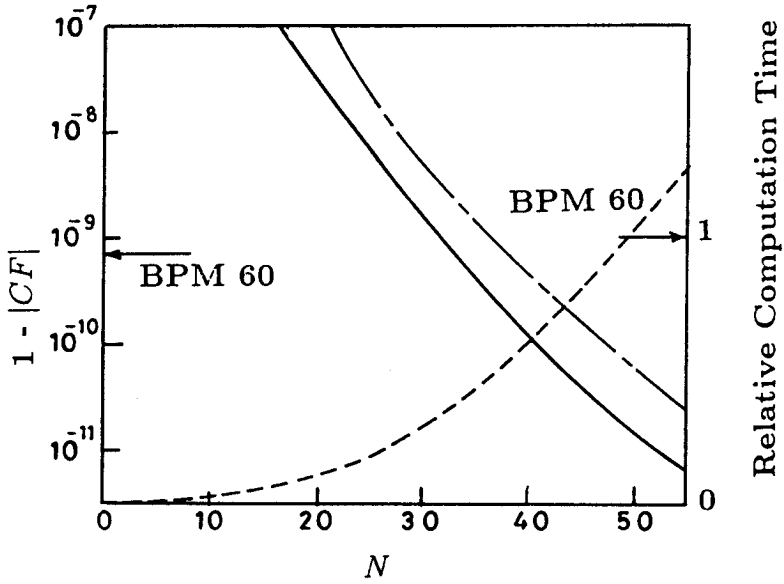

Figure 10. The error in the correlation factor, 1-$|CF|$, as a function of the number of collocation points, N, for a uniform 3-D waveguide defined by the refractive index distribution given in Eq. 69, using the OCM with the cartesian coordinates (Sec. 6.1) and the circular coordinates (Sec. 6.2) shown by the continuous and the dash-dot curves respectively. The dashed curve shows the relative computation time for the OCM with the cartesian coordinates (Sec. 6.1). The corresponding quantities for the 3-D BPM with 60 sample points are also shown.

	The BPM	The OCM
$2-D$	$m(4\log_2 m+1)$	$4N^2$
$3-D$	$m^2(8\log_2 m+1)$	$4N^2(2N+1)$
Increment Factor	$2m$	$2N$
$(m, N \gg 1)$		

*m and N are the number of sample points in the BPM and the collocation method (OCM), respectively.

Table 1. Number of multiplications in one propagation step. m and N are the number of sample points in the BPM and the collocation method (OCM), respectively.

7. Applications of the Collocation Equation

It has been shown in Sec. 2.1 that the Helmholtz equation (Eq. 2) can be converted into a second order matrix differential equation and that the "equivalence" between these two equations becomes increasingly accurate as the size of the matrices, N, increases. In this respect, the collocation method differs radically from the BPM, in which no such equation can be obtained. The advantages of obtaining such an equation are many fold. Firstly, one can use different approaches to solve the resulting equation. Indeed, we have used the Runge-Kutta method in Sec. 2.3, whereas a matrix operator method is used in Sec. 3. Secondly, one can use special methods to solve certain specific problems. As an example, we discuss in the next section a special method for periodic waveguides where one has to solve the second order equation directly due to the presence of reflected waves. Another method that can be used for solving a differential equation is the perturbation technique when the longitudinal variation of the refractive index is weak. As an example, we consider, in Sec. 7.2, wave propagation through weakly random waveguides. Finally, the collocation equation can be easily converted into a matrix eigenvalue equation for modes of a uniform waveguide (see Sec. 7.3).

7.1 Periodic Waveguides

Periodic optical waveguides have attracted a considerable amount of interest both for theoretical and numerical studies because of their numerous applications in Distributed Bragg Reflector (DBR)[41] and Distributed Feedback (DFB) [42] lasers, beam steering devices, and as input and output couplers.

Periodic waveguides have been analyzed by various numerical techniques [43–45]. The coupled mode formulation [44] is the most commonly used method. The coupled mode formulation in its complete form can yield exact results. However, the analysis becomes complicated because of the presence of radiation modes. The main assumptions of the coupled mode formulation include (i) retaining only one scattered wave in addition to the fundamental mode, and (ii) neglecting second derivatives of the field amplitudes. With these assumptions, one is able to obtain simple, analytical expressions.

In the collocation method, full beam, including guided as well as radiation modes, are taken into account [46]. However, as mentioned above, in periodic structures one cannot make the Fresnel approximation, due to the presence of the strong coupling to the backward propagating wave. It is for this reason that the Beam Propagation Method cannot be used for the study of periodic waveguides. Here we have considered the full second order Helmholtz equation, and hence, we have to solve the second order collocation equation, Eq. 18.

In the case of periodic waveguides, $\mathbf{R}(z)$ varies periodically with z. We look for analytical solutions of Eq. 18 by writing it in the following form

$$d\Phi/dz = \mathcal{H}(z)\Phi(z) \tag{70}$$

where Φ is a vector of dimension $2N \times 1$ and is defined as

$$\Phi = \begin{bmatrix} \Psi \\ d\Psi/dz \end{bmatrix} \tag{71}$$

and $\mathcal{H}$ is a $2N \times 2N$ square matrix defined as

$$\mathcal{H}(z) = \begin{bmatrix} \mathbf{0} & \mathbf{I} \\ -\mathbf{S} & \mathbf{0} \end{bmatrix}. \tag{72}$$

$\mathcal{H}(z)$ is a periodic function of z, since $\mathbf{R}(z)$ and, hence, $\mathbf{S}(z)$ are periodic in z. Thus, we have

$$\mathcal{H}(z + \Lambda) = \mathcal{H}(z) \tag{73}$$

where Λ is the period along z. We have to solve Eq. 70 with a given initial condition, say $\Phi(0) = \Phi_0$. One begins by solving an auxiliary equation [47]

$$d\mathcal{F}/dz = \mathcal{H}(z)\mathcal{F}(z) \tag{74}$$

where $\mathcal{F}(z)$ is a square matrix such that $\mathcal{F}(0) = \mathbf{I}$. The solution of Eq. 70 can then be written as

$$\Phi(z) = \mathcal{F}(z)\Phi_0 \tag{75}$$

Assuming that $\mathcal{H}(z)$ is continuous and periodic function of z, the solution of Eq. 74 can be written as [47]

$$\mathcal{F}(z) = \mathcal{L}(z)\exp(\mathcal{M}z) \tag{76}$$

where the matrix $\mathcal{L}(z)$ is a periodic function of z with the same period as that of $\mathcal{H}$, and $\mathcal{M}$ is a constant square matrix. In order to compute $\mathcal{L}(z)$ and $\mathcal{M}$, one has to solve the matrix differential equation (Eq. 74) over one period, Λ. Thus, if the field after one period, $\mathcal{F}(\Lambda)$, is known, Eq. 76 gives

$$\mathcal{F}(\Lambda) = \exp(\mathcal{M}\Lambda) \tag{77}$$

so that $\mathcal{M}$ is given as

$$\mathcal{M} = \ln[\mathcal{F}(\Lambda)]/\Lambda \tag{78}$$

and $\mathcal{L}(z)$, which is a periodic function, is given by

$$\mathcal{L}(z) = \mathcal{F}(z)\exp(-\mathcal{M}z), \qquad 0 \leq z \leq \Lambda \tag{79}$$

The solution of the auxiliary equation is then given by

$$\mathcal{F}(z) = \mathcal{L}(z - \Lambda.\text{int}[z/\Lambda])\exp(\mathcal{M}z) \tag{80}$$

where int[ ] represents the integer part of the argument. Finally using Eq. 75, one can obtain $\Phi(z)$. The natural logarithm of a matrix is computed by diagonalization.

The above procedure is valid when the waveguide is strictly periodic. In case of gratings with axially varying parameters [48] and other structures in which there is coupling into the backward wave, but there is no periodicity, one would have to solve Eq. 18 directly using, say, the Runge-Kutta method.

In structures with reflections, the boundary condition at $z = 0$ is not known due the presence of the reflected wave. However, if the length of the periodic structure is L, which implies that there are no reflections possible after $z = L$, then one can construct, with reasonable accuracy, a boundary condition at $z = L$. One can then propagate the wave in the backward direction, from $z = L$ to $z = 0$ and obtain the wave at $z = 0$ which is composed of both the reflected and the forward propagating waves. From this wave one can obtain, the power in the forward and backward propagation modes and calculate the modal reflection coefficient. The procedure would become apparent from the example given below.

We consider a periodic waveguide of length L with a sech^2-profile and a periodicity due to the variation of the half-width of the waveguide. Thus,

$$n^2(x,z) = n_2^2 + (n_1^2 - n_2^2)\mathrm{sech}^2[x/a(z)] \tag{81}$$

with

$$a(z) = a_0 + b_0 \cos(2\pi z/\Lambda) \tag{82}$$

We have chosen the following parameters: $n_1 = 1.567, n_2 = 1.513, a_0 = 1.5\,\mu\mathrm{m}$, $\Lambda = 0.1683\,\mu\mathrm{m}$, $b_0 = 0.8\,\mu\mathrm{m}$ and $\lambda_0 = 0.5658\,\mu\mathrm{m}$.

In our calculations, we begin with the condition that at $z = L$, only the forward propagating fundamental mode exists. Thus,

$$\psi(x,L) = \psi_0(x) \equiv \cosh^{-W}(x/a_0) \tag{83}$$

and

$$\left.\frac{\partial\psi(x,z)}{\partial z}\right|_{z=L} = -i\beta\psi(x,L) \tag{84}$$

β being the propagation constant of the mode and $W = a_0\sqrt{\beta^2 - k_0^2 n_2^2}$. We then calculate the field and its first derivative at $z=0$ using the procedure described above. The propagation over one period is obtained using the Runge-Kutta method for Eq. 74. At $z=0$, the field comprises of a forward propagating mode with amplitude, A_+, and a backward propagating mode with amplitude, A_-. Hence, we can write

$$\psi(x, z=0) = A_+\psi_0 + A_-\psi_0 + \text{contribution of radiation modes} \tag{85}$$

and

$$\left.\frac{\partial\psi(x,z)}{\partial z}\right|_{z=0} = -i\beta A_+\psi_0 + i\beta A_-\psi_0 + \text{contribution of radiation modes} \tag{86}$$

Using the orthogonality of the guided and radiation modes, we obtain

$$A_+ = \frac{\int \psi(x, z=0)\psi_0 dx + (i/\beta) \int \left.\frac{\partial \psi}{\partial z}\right|_{z=0} \psi_0 dx}{2 \int |\psi_0|^2 dx} \tag{87}$$

and

$$A_- = \frac{\int \psi(x, z=0)\psi_0 dx - (i/\beta) \int \left.\frac{\partial \psi}{\partial z}\right|_{z=0} \psi_0 dx}{2 \int |\psi_0|^2 dx} \tag{88}$$

Thus, the modal reflection coefficient may be calculated as

$$R = |A_-|^2 / |A_+|^2 .$$

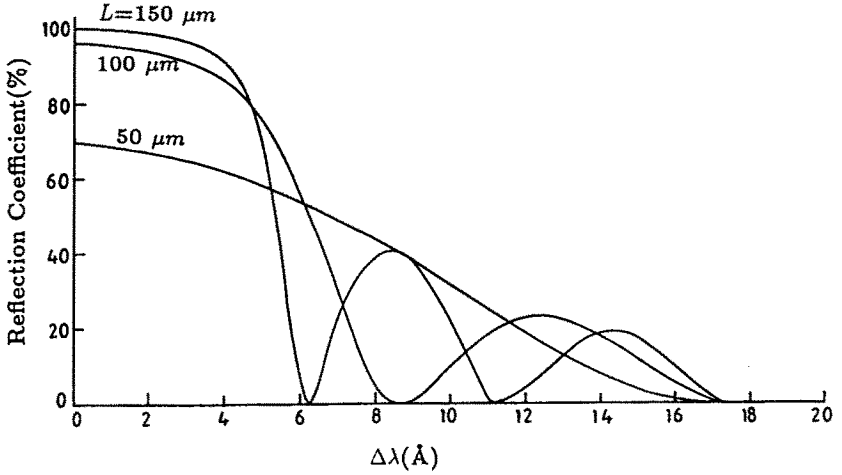

Figure 11. Reflection coefficient for the fundamental mode as a function wavelength, $\lambda - \lambda_0 = \Delta\lambda$, in a periodic waveguide defined in Eqs. 81 and 82 for different lengths, L, of the periodic corrugations.

With the above procedure, we were able to obtain [46] the typical variation of the reflection coefficient as a function of $\Delta\lambda = \lambda - \lambda_0$

shown in Fig. 11 for different values of the length L. The curves are very similar to those obtained using the coupled mode theory [49]. In the above example, we have neglected the presence of radiation modes at and after $z = L$. However, in propagating the field from $z = L$ to $z = 0$, the radiation modes are included. One can, therefore, estimate the power coupled into radiation and other modes by calculating the difference integral

$$\frac{\int |\psi(x, z = 0) - (A_+ + A_-)\psi_0|^2 \, dx}{2 \int |\psi(x, z = 0)|^2 \, dx}$$

In the above example, it was found that the power coupled into these modes is between $0.1 - 0.2\%$ for the given wavelength range.

7.2 Waveguides with Random Variations

Next, we consider an application in which the perturbation-type of expansion is used to obtain the effect of z-dependent variation in the refractive index on wave propagation. In particular, we consider a planar waveguide with weak random index variations:

$$n^2(x, z) = n_2^2 + (n_1^2 - n_2^2) f(x)[1 + \delta\xi(z)] \tag{89}$$

where $f(x)$ defines the index profile and $\xi(z)$ is a random function of z. The parameter δ defines the strength of randomness in the refractive index and we consider that $\delta \ll 1$.

Propagation of waves in a random medium has been a subject of extensive investigations. Amongst the various theories that have been developed, the moment method [50], in which one directly obtains equations describing the evolution of the correlation function of the electric field, appears to be the most elegant method. The second moment equation, solution of which determines the average intensity distribution across the beam profile, is easily solved. The fourth moment equation, which contains information about the intensity fluctuations and intensity correlations, is more difficult to analyze. The fourth moment equation has been studied by perturbation [51,52], asymptotic [53,54] and numerical techniques [55–57]. An alternative approach is to solve the stochastic wave equation directly by Monte Carlo techniques [58]; the obvious drawback being that a large computational effort is

required if reasonably accurate estimates of the moments of the field are required.

Comparatively fewer studies have been made on optical waveguides with random inhomogeneities. In this case, the governing equations become much more complicated. Goyal *et al.* [59] and Sharma *et al.* [60] have studied fluctuations in the beam width parameter, and mode conversion for Gaussian beams in random square law media. Propagation of Gaussian beams in square law media has been analytically studied by Papanicoloaou *et al.* [61] and they have obtained expressions for average beam intensity and intensity fluctuations, but no expressions for the these quantities have been obtained for general waveguiding structures. Crosignani *et al.* [62] have developed a set of statistical coupled equations for second and fourth moments of the mode amplitude in a fiber for studying mode coupling and evaluation of cross-correlation between powers of different modes; but, these expressions become very complicated if one has to take radiation modes into account.

We show here briefly that the collocation method can be used for a numerical study [17] of wave propagation in waveguides with random perturbations in the refractive index, such as the one defined in Eq. 89 above. The Helmholtz equation for the refractive index of Eq. 89 can be converted into the following matrix differential equation (see Sec. 2.1 for details)

$$\frac{d^2\Psi}{dz^2} + [\mathbf{B}\mathbf{A}^{-1} + \mathbf{R}(z)]\Psi(z) = 0 \tag{90}$$

which on using the Fresnel approximation reduces to a first order equation (*cf.* Eq. 22)

$$\frac{d\mathcal{X}}{dz} = [\mathbf{B}\mathbf{A}^{-1} + \mathbf{R}(z) - k^2\mathbf{I}]\mathcal{X}(z)/2ik \equiv -i\mathcal{G}\mathcal{X} - i\delta\xi(z)\mathcal{D}\mathcal{X} \tag{91}$$

where $\mathcal{G} \equiv (\mathbf{B}\mathbf{A}^{-1} + \mathbf{R}_0 - k^2\mathbf{I})/2k$ is a constant matrix and $\mathbf{R}(z)$ has been written as a sum of a deterministic part, $\mathbf{R}_0$ and a stochastic part:

$$\mathbf{R}(z) = \mathbf{R}_0 + \delta\xi(z)\mathcal{D} \tag{92}$$

with

$$\mathcal{D} = k_0^2(n_1^2 - n_2^2) \times \text{diag.}\{f(x_1) \quad f(x_2) \quad \ldots \quad f(x_N)\} \tag{93}$$

In order to solve Eq. 91, we consider following expansion in orders of δ:

$$\mathcal{X} = \mathcal{X}_0 + \delta\mathcal{X}_1 + \delta^2\mathcal{X}_2 + \ldots \tag{94}$$

which when used in Eq. 91 gives the following equations for different expansion terms:

$$\frac{d\mathcal{X}_0}{dz} = -i\mathcal{G}\mathcal{X}_0 \tag{95}$$

$$\frac{d\mathcal{X}_1}{dz} = -i\mathcal{G}\mathcal{X}_1 - i\xi(z)\mathcal{D}\mathcal{X}_0 \tag{96}$$

$$\frac{d\mathcal{X}_2}{dz} = -i\mathcal{G}\mathcal{X}_2 - i\xi(z)\mathcal{D}\mathcal{X}_1 \tag{97}$$

The solution of Eq. 95 can be obtained analytically as

$$\mathcal{X}_0(z) = \exp[-i\mathcal{G}z]\ \mathcal{X}_0(0) \tag{98}$$

Further, solutions to Eqs.96 and 97 can be written as

$$\mathcal{X}_1(z) = -i\int^z \xi(z')\exp[-i\mathcal{G}(z-z')]\mathcal{D}\mathcal{X}_0(z')dz' \tag{99}$$

$$\mathcal{X}_2(z) = -i\int^z \xi(z')\exp[-i\mathcal{G}(z-z')]\mathcal{D}\mathcal{X}_1(z')dz' \tag{100}$$

The averages of quantities $\mathcal{X}_0$, $\mathcal{X}_1$ and $\mathcal{X}_2$ and their products can be expressed as finite sums over simple functions such as exponentials of the elements of the various matrices involved. The algebra is simplified if the field at $z = 0$ is a mode of the waveguide. Using this procedure, we can find the expressions for the moments of the field and ensemble averages of various important quantities such as, the electric field, field intensity and intensity fluctuations. The details of these computations are given elsewhere [17]. The analysis can also be applied to uniform medium with random fluctuations in the refractive index.

7.3 Evaluation of Modes of Uniform Waveguides

Although the main application of the collocation method is in the study of structures nonuniform in the direction of propagation, it can

also be used simply and effectively for obtaining the modes of a waveguide. In case of uniform waveguides, the orthogonal collocation method results in a matrix eigenvalue equation, the solution of which yields the propagation constants and modal field distributions. We have solved this eigenvalue problem for different planar waveguides and have shown that the accuracies obtained using the collocation method are comparable to those obtained using the Galerkin method for the same number of basis functions and the computational effort taken is much less [9]. However, in case of refractive index profiles with a discontinuity, the collocation method yields poorer results for the propagation constant which can be improved by a simple perturbative correction.

We again consider the collocation equation, Eq. 18. For a mode in a uniform waveguide, $\Psi(z)$ can be written as $\Psi_0 \exp(-i\beta z)$, where Ψ_0 represents the modal field pattern at the collocation points, which remains unchanged along the length of the waveguide, and β is the propagation constant. Substituting this form for $\Psi(\mathbf{z})$ in the matrix differential equation, Eq. 18, we obtain

$$\mathbf{S}\Psi_0 = \beta^2 \Psi_0 \tag{101}$$

which is a standard matrix eigenvalue equation. $\mathbf{S}$ is a real but not symmetric matrix. However, by a similarity transformation, which leaves the eigenvalues of $\mathbf{S}$ unchanged, it can be transformed into a real symmetric matrix (See Appendix A for details). Thus, the eigenvalues and eigenvectors are all real and since the evaluation of eigenvalues for a symmetric matrix is much simpler, the computational effort required is also considerably reduced.

A number of numerical examples are given in Ref. [9] and we will not include any example here. We would, however, like to add that in the collocation method, it is also possible to take advantage of the variable transformation in evaluation of the propagation constant.

8. Application to Nonlinear Pulse Propagation through Optical Fibers

8.1 Generalized Nonlinear Schrödinger Equation

It is well known that the effect of pulse dispersion in optical fibers can be reduced by the use of the nonlinear Kerr effect as proposed by

Hasegawa and Tappert [63] and experimentally verified by Mollenauer et al. [64]. A large number of interesting nonlinear phenomena occur in optical fibers due to the interplay of nonlinear and dispersive effects. Under some specific conditions solitons exist; solitons are pulses with specific shapes which travel undistorted for extremely large distances as a result of balance between nonlinear and dispersive effects in a fiber (see, e.g., [65,66]).

The nonlinear evolution of short pulses in an optical fiber is usually described by the nonlinear Schrödinger equation (NLS) which has been analytically solved [67]. The NLS equation holds good for pulses of picosecond duration. However, some assumptions implicit in the equation are no longer valid for pulses of smaller duration, particularly, in the femtosecond regime. Hence, the NLS equation has to be modified to include a host of other phenomena, such as higher order dispersion, higher order nonlinearities, attenuation and self-steepening. Thus, in presence of Kerr-like nonlinearity, pulse propagation can be described by the Generalized Nonlinear Schrödinger Equation (GNLSE) [65,68]

$$i\frac{\partial E}{\partial \xi} + i\gamma E + \frac{\partial^2 E}{\partial \tau^2} - i\delta\frac{\partial^3 E}{\partial \tau^3}$$
$$= -[|E|^2 E + is\frac{\partial}{\partial \tau}(|E|^2 E) - \tau_R E\frac{\partial}{\partial \tau}(|E|^2)] \qquad (102)$$

where it is assumed that the pulse is propagating in the region of anomalous dispersion ($\beta_2 \equiv d^2\beta/d\omega^2 < 0$). The space and time variables are normalized such that

$$\xi = z\,|\beta_2|\,/T_0^2;$$
$$\tau = \sqrt{2}T/T_0; \qquad (103)$$
$$T = t - \beta_1 z$$

where T represents the reduced time (measured from the pulse center), T_0 is the width of the pulse and $\beta_1 = d\beta/d\omega$ is the inverse of the group velocity of the pulse. In Eq. 102, $E(z,t)$ denotes the envelope of the electric field and is assumed to be a slowly varying function of z and t:

$$\psi(z,t) = E(z,t)e^{i(\omega t - \beta z)} \qquad (104)$$

Further, in Eq. 102, γ is the attenuation coefficient and the parameters δ, s and τ_R represent, respectively, the effect of higher order dispersion, self-steepening and the retarded nonlinear response. Explicitly, these can be written as

$$\begin{aligned} \delta &= \sqrt{2}\beta_3/3\,|\beta_2|\,T_0, \\ s &= 2\sqrt{2}/\omega_0 T_0 \\ \tau_R &= \sqrt{2}T_R/T_0 \end{aligned} \tag{105}$$

where $\beta_3 = d^3\beta/d\omega^3$ is the third order dispersion parameter and T_R is related to the slope of the Raman gain in the fiber [65]. All these parameters δ, s and τ_R vary inversely with the pulse width and are negligible for pulses with $T_0 > 1$ ps, and become appreciable for pulses in the femtosecond regime.

Analytic solutions of Eq. 102 are possible only for few specific cases and in most cases, the GNLSE has to be solved numerically. The numerical method commonly used to solve the GNLSE is the split-step Fourier method [65,69], which is in fact a form of the BPM. This type of procedure has some inherent drawbacks. One has to use numerical differentiation in evaluating terms containing derivatives of the pulse envelope. Further, the effects of nonlinearity and dispersion are assumed to be separated in space, whereas in reality both act simultaneously. The collocation method does not suffer from these drawbacks and the numerical examples show that the collocation method is considerably more efficient even for solving GNLSE.

8.2 Collocation Method for the GNLSE

We begin by expressing the pulse envelope $E(\xi,\tau)$ as a linear combination of the Hermite-Gauss functions, $\varphi_n(\tau) = H_{n-1}(\alpha\tau)\exp(-\alpha^2\tau^2/2)$:

$$E(\xi,\tau) = \sum_{n=1}^{N} c_n(\xi)\varphi_n(\tau) \tag{106}$$

α being the width parameter. The collocation points are now defined as the N zeroes of $H_N(\alpha\tau)$. Applying the collocation principle as described in Sec. 2.1, Eq. 102 can be converted into the following matrix differential equation:

$$i\frac{d\mathbf{E}}{d\xi} + i\gamma\mathbf{E} + \hat{\mathbf{B}}\hat{\mathbf{A}}^{-1}\mathbf{E} - i\delta\hat{\mathbf{D}}\hat{\mathbf{A}}^{-1}\mathbf{E}$$
$$= -[\hat{\mathbf{P}}\mathbf{E} + is(\hat{\mathbf{Q}}\hat{\mathbf{F}}\hat{\mathbf{A}}^{-1}\mathbf{E}^* + 2\hat{\mathbf{P}}\hat{\mathbf{F}}\hat{\mathbf{A}}^{-1}\mathbf{E})]$$
$$- \tau_R(\hat{\mathbf{Q}}\hat{\mathbf{F}}\hat{\mathbf{A}}^{-1}\mathbf{E}^* + \hat{\mathbf{P}}\hat{\mathbf{F}}\hat{\mathbf{A}}^{-1}\mathbf{E}) \tag{107}$$

where $\mathbf{E}(\xi)$ is a column vector of the values of $E(\xi, \tau_j)$ at consecutive collocation points τ_j and $\hat{\mathbf{P}}$ and $\hat{\mathbf{Q}}$ are diagonal matrices with the successive diagonal elements being $|E(\xi, \tau_j)|^2$ and $E^2(\xi, \tau_j)$, respectively. The elements of the $N \times N$ matrices $\hat{\mathbf{A}}, \hat{\mathbf{B}}, \hat{\mathbf{D}}$ and $\hat{\mathbf{F}}$ are defined as:

$$\hat{A}_{jn} = \varphi_n(\tau_j)$$
$$\hat{B}_{jn} = \left.\frac{d^2\varphi_n}{d\tau^2}\right|_{\tau=\tau_j}$$
$$\hat{D}_{jn} = \left.\frac{d^3\varphi_n}{d\tau^3}\right|_{\tau=\tau_j}$$
$$\hat{F}_{jn} = \left.\frac{d\varphi_n}{d\tau}\right|_{\tau=\tau_j} \tag{108}$$

Various derivatives of $\varphi_n(\tau)$ can be analytically evaluated using the recurrence formulae for $H_n(\tau)$ [25]. The matrix equation, Eq. 107, is solved using the Runge-Kutta method starting from the given pulse shape $E(\xi = 0, \tau)$ at $\xi = 0$.

8.3 Numerical Example

To establish the accuracies obtainable using the collocation method, we consider an example for which an analytical solution is known. Neglecting the effects of loss, third order dispersion, self steepening and the retarded nonlinear response, Eq. 102 reduces to the nonlinear Schrödinger (NLS) equation:

$$i\frac{\partial E}{\partial \xi} + \frac{\partial^2 E}{\partial \tau^2} + |E|^2 E = 0 \tag{109}$$

which gives solitons as its solutions. The fundamental soliton has an initial pulse shape defined by (see, e.g., [65])

$$E(\xi = 0, \tau) = \text{sech}(\tau/\sqrt{2}) \tag{110}$$

In our example, we have propagated this pulse using the collocation method upto $\xi = 2$ and have calculated the correlation factor (CF) of the output pulse amplitude with the input pulse amplitude:

$$CF = \frac{\int E^*(\xi = 2, \tau)\ E(\xi = 0, \tau)\ d\tau}{\sqrt{\int |E(\xi = 2, \tau)|^2\, d\tau . \int |E(\xi = 0, \tau)|^2\, d\tau}} \tag{111}$$

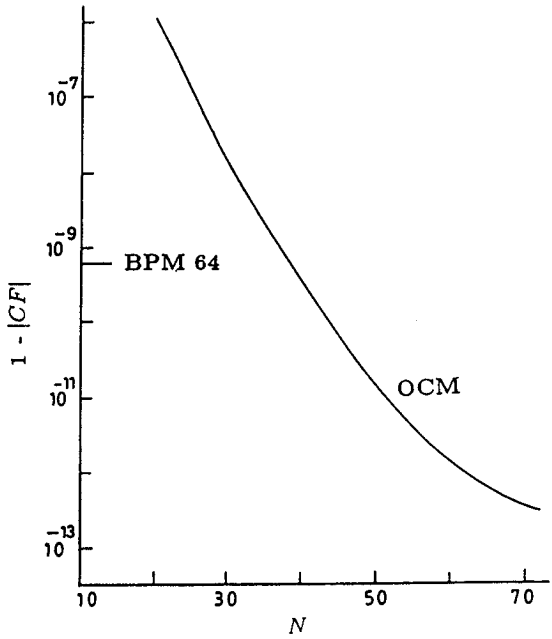

Figure 12. The error in the correlation factor, 1-$|CF|$, (Eq. 111) as a function of the number of collocation points, N, after propagation of the fundamental soliton through a distance, ξ =2, using the collocation method (OCM). Also shown is the error in the BPM with 64 sample points.

Ideally the absolute value of the correlation factor should be equal to unity since only phase changes with ξ. The deviation of the absolute value of the correlation factor from unity gives a measure of the error in the method of propagation. We have plotted this error as a function of the number of collocation points in Fig. 12. We have performed the same computations using the split-step Fourier method (BPM). We see that the accuracy of little over 10^{-9}, obtained by using 64 BPM points, can be obtained by using 35 collocation points and the computation time required is about half. On the other hand, in about the same amount of computation time (*i.e.*, with $N = 50$, since, in the collocation method the computation time increases as N^2), an improvement in accuracy by about two orders of magnitude can be obtained.

More examples on pulse propagation including the effects of higher order dispersion, self-steepening and retarded response are included in Refs. [15,16].

9. Summary

In conclusion, we have described the collocation method for propagation of optical fields through waveguiding structures and have presented some numerical examples for demonstrating the validity of the methods presented and for comparing wherever possible with the commonly used Beam Propagation Method (BPM).

We have shown through examples that the collocation method has a substantial computational advantage over the BPM. The collocation method converts the Helmholtz equation into a matrix differential equation and the accuracy of this matrix representation can, in principle, be improved in an unlimited fashion as the size of the matrices involved increases. This, however, increases the computational effort involved and one generally has to make a compromise between the accuracy obtained and the computational effort put in. For a desired accuracy, the computational effort in the collocation method is substantially smaller (typically by a factor of about two or more) in comparison to the BPM. In addition, there are several advantageous features in the collocation method that cannot be implemented in the methods like the BPM. We have shown, for example, that a variable transformation in the collocation method can be used to improve accuracy by orders of magnitude for a given computational effort. Another

feature is that one can choose the set of basis functions which is suitable for the given problem. Thus, while for planar waveguiding problems the Hermite-Gauss functions are better, the sinusoidal functions are better suited for the study of the propagation problems in homogeneous media.

As mentioned above, the collocation method results in a matrix differential equation (which has been termed as the collocation equation); this is a great advantage, since this equation can be solved in a variety of ways depending on the problem at hand. One could solve it using a direct method like the Runge-Kutta method or the predictor-corrector method [25,27], or, by using matrix operator algebra, or, by using a perturbative approach wherever applicable. For homogeneous media, even analytical solutions are possible.

Unlike in the BPM, the collocation method retains the second order differentials of the Helmholtz equation. This allows the use of the collocation equation for waveguiding problems in which reflections are involved. Indeed, we have shown that the propagation through a periodic structure can be treated very elegantly in a semi-analytical fashion using the collocation method.

The collocation method is general enough to be applicable to other propagation problem not based on the Helmholtz equation. We have used this method to solve the generalized nonlinear Schrödinger equation to model nonlinear pulse propagation through optical fibers. It can also be similarly applied to nonlinear propagation problems in planar waveguides.

There are, however, a number of aspects connected with the collocation method which are still to be investigated. The behavior of the field at the edge of the computation window (the last collocation point in this case), particularly in comparison to the BPM, needs a detailed study. Problem of reflection from nonperiodic structures can also be handled, but is still to be demonstrated. Extension to solution of vector wave equation remains to be explored. Like any other method based on basis functions, which along with their derivatives are continuous, the collocation method also runs into some difficulty while being used for step-index profiles. Change of variable to crowed sampling points around the step is likely to improve accuracy, but this remains to be explored. Further, higher order split-step methods which have recently been used for the BPM [70–72] can be implemented in a straightforward manner for the collocation method.

Acknowledgements

The author would like to express his gratitude to Professor A.K. Ghatak for numerous enlightening discussions held and for the encouragement he provided during the course of development of the collocation method. He would also like to acknowledge the vital inputs provided by Dr. Swagata Deb (née Banerjee) and Dr. Anju Nayyar (née Taneja) to the developments of the collocation method mainly as doctoral students. Thanks are also due to Dr. Mukesh P. Singh for his help in preparation of this manuscript. A substantial part of this work was supported through a Homi Bhabha Fellowship to the author. The work covered in this chapter was partially supported by grants from the Council of Scientific and Industrial Research (India) and from the National Institute of Standards and Technology (USA) and the Department of Science and Technology (India).

Appendix A: Properties of Matrices A and S.

We derive, in this Appendix, some of the properties of matrices **A** and **S**. The matrix **A** is defined in Eq. 14. The Hermite-Gauss functions, $\phi_n(x)$ are the functions used in the Gaussian quadrature procedure over the interval ∞ to $-\infty$ [25,26]. In this procedure, an integral over an infinite domain can be *exactly* converted into a finite summation if the integrand satisfies certain conditions. Using this property, we can write

$$\int_{-\infty}^{\infty} \phi_n(u)\phi_m(u)du = \sum_{j=1}^{N} W_j^2 \phi_n(u_j)\phi_m(u_j)du = \delta_{nm}$$

where $u = \alpha x$ and W_j^2 are the weight functions tabulated in the Gaussian quadrature tables [25,26]. The integral on the left side is equal to the Kronecker delta, δ_{ij} because the functions $\phi_n(u)$ are orthonormal to each other. The summation in the above equation can be written in terms of matrices as

$$(\mathbf{WA})^T(\mathbf{WA}) = \mathbf{I}$$

where **W** is a diagonal matrix with $W_1, W_2, \ldots, W_N$ as its diagonal elements. With simple manipulations, this equation can be written as

$$\mathbf{A}\mathbf{A}^T = (\mathbf{W}\mathbf{W}^T)^{-1}$$

which gives an analytical expression for the inverse of $\mathbf{A}$

$$\mathbf{A}^{-1} = \mathbf{A}^T(\mathbf{W}\mathbf{W}^T) = \mathbf{A}^T\mathbf{W}^2$$

Thus, the inverse of $\mathbf{A}$ can be found by simply multiplying the transpose of $\mathbf{A}$ by a known diagonal matrix $\mathbf{W}^2$.

The functions $\phi_n(u)$ satisfy the following differential equation [25]

$$\frac{d^2\phi_n}{du^2} = [u^2 - (2n-1)]\phi_n(u)$$

and, hence, the elements of matrix $\mathbf{B}$, defined in Eq. 16, can be written as

$$B_{jn} = \alpha^2[u_j^2 - (2n-1)]A_{jn}$$

which, in the matrix form, can be written as

$$\mathbf{B} = \mathbf{D}_1\mathbf{A} - \mathbf{A}\mathbf{D}_2$$

where $\mathbf{D}_1$ and $\mathbf{D}_2$ are defined in Eq. 28. The matrix $\mathbf{S}$ can now be written as

$$\mathbf{S} = \mathbf{D}_1 + \mathbf{R} - \mathbf{A}\mathbf{D}_2\mathbf{A}^{-1} = \mathbf{D}_4 - \mathbf{A}\mathbf{D}_2\mathbf{A}^{-1}$$

where $\mathbf{D}_4$ is a diagonal matrix. Now, we make a similarity transformation of $\mathbf{S}$ by $\mathbf{A}$ to obtain

$$\mathbf{S}' \equiv \mathbf{A}^{-1}\mathbf{S}\mathbf{A} = \mathbf{A}^{-1}\mathbf{D}_4\mathbf{A} - \mathbf{D}_2$$

We have seen above that $\mathbf{A}\mathbf{A}^T$ is a diagonal matrix and since all diagonal matrices commute with each other, we can write

$$\begin{aligned}\mathbf{D}_4 &= (\mathbf{A}\mathbf{A}^T)\mathbf{D}_4(\mathbf{A}\mathbf{A}^T)^{-1} \\ \mathbf{A}^{-1}\mathbf{D}_4\mathbf{A} &= \mathbf{A}^T\mathbf{D}_4(\mathbf{A}^T)^{-1} \\ &= (\mathbf{A}^{-1}\mathbf{D}_4\mathbf{A})^T\end{aligned}$$

which shows that $\mathbf{A}^{-1}\mathbf{D}_4\mathbf{A}$ is a symmetric matrix and hence, $\mathbf{S}'$ is also a real symmetric matrix. Thus, the eigenvalues and eigenvectors of $\mathbf{S}'$ and $\mathbf{S}$ are all real.

Appendix B: Properties of Matrix $\hat{\mathbf{H}}_2$.

We show, in this Appendix, that the matrix $\hat{\mathbf{H}}_2$ defined in Eq. 48 is similar to a real symmetric matrix. The matrix $\hat{\mathbf{D}}_2$ is a positive definite diagonal matrix and hence, we can write it as a square of another diagonal matrix $\mathbf{D}$, whose diagonal elements are square roots of the corresponding elements of $\hat{\mathbf{D}}_2$. Thus,

$$\begin{aligned}
\hat{\mathbf{H}}_2 &= \mathbf{F}\mathbf{A}\mathbf{D}^2\mathbf{A}^{-1}, \\
\mathbf{A}^{-1}\hat{\mathbf{H}}_2\mathbf{A} &= \mathbf{A}^{-1}\mathbf{F}\mathbf{A}\mathbf{D}^2, \\
\mathbf{D}\mathbf{A}^{-1}\hat{\mathbf{H}}_2\mathbf{A}\mathbf{D}^{-1} &= \mathbf{D}\mathbf{A}^{-1}\mathbf{F}\mathbf{A}\mathbf{D}, \\
(\mathbf{D}\mathbf{A}^{-1})\hat{\mathbf{H}}_2(\mathbf{D}\mathbf{A}^{-1})^{-1} &= \mathbf{D}\mathbf{A}^T\mathbf{W}^2\mathbf{F}\mathbf{A}\mathbf{D},
\end{aligned}$$

where we have used $\mathbf{A}^{-1} = \mathbf{A}^T\mathbf{W}^2$. The matrix on the right hand side of the last equation above is a symmetric matrix, since apart from $\mathbf{A}$, all other matrices are diagonal matrices which are symmetric and commute with each other. This proves that the matrix $\hat{\mathbf{H}}_2$ is similar to a real symmetric matrix.

References

1. Fleck, J. A.,Jr., J. R. Morris, and M. D. Feit, "Time-dependent propagation of high energy laser beams through the atmosphere," *Appl. Phys.*, Vol. 10, 129–160, 1976.
2. Feit, M. D., and J. A. Fleck, Jr., "Light propagation in graded-index optical fibers," *Appl. Opt.*, Vol. 17, 3990–3998, 1978.
3. Feit, M. D., and J. A. Fleck, Jr., "Calculation of dispersion in graded-index multimode fibers by a propagating beam method," *Appl. Opt.*, Vol. 18, 2843–2851, 1979.
4. Feit, M. D., and J. A. Fleck, Jr., "Computation of mode properties in optical fiber waveguides by a propagating beam method," *Appl. Opt.*, Vol. 19, 1154–1166, 1980.
5. Feit, M. D., and J. A. Fleck, Jr., "Computation of mode eigenfunctions in graded-index optical fibers by the propagating beam method," *Appl. Opt.*, Vol. 19, 2240–2246, 1980.
6. Feit, M. D., and J. A. Fleck, Jr., "Mode properties of optical fibers with lossy components by the propagating beam method," *Appl. Opt.*, Vol. 20, 848–856, 1981.

7. Feit, M. D., and J. A. Fleck, Jr., "Analysis of rib waveguides and couplers by the propagating beam method," *J. Opt. Soc. Am. A*, Vol. 7, 73–79, 1990.
8. Sharma, A., and S. Banerjee, "Method for propagation of total fields or beams through optical waveguides," *Opt. Lett.*, Vol. 14, 94–96, 1989.
9. Banerjee, S., and A. Sharma, "Propagation characteristics of optical waveguiding structures by direct solution of the Helmholtz equation for total fields," *J. Opt. Soc. Am. A*, Vol. 6, 1884–1894, 1989; Errata: Vol. 7, 2156, 1990.
10. Sharma, A., and A. Taneja, "Unconditionally stable formulation of the collocation method," Presented at the *Integrated Photonics Research* Meeting of the Optical Society of America, Monterey (California, USA), April 9–11, 1991. Paper # TuB4.
11. Sharma, A., and A. Taneja, "Unconditionally stable procedure to propagate beams through optical waveguides using the collocation method," *Opt. Lett.*, Vol. 16, 1162–1164, 1991.
12. Sharma, A., and A. Taneja, "Variable-transformed collocation method for field propagation through waveguiding structures," *Opt. Lett.*, Vol. 17, 804–806, 1992.
13. Sharma, A., and A. Taneja,"Collocation method for field propagation through optical waveguides: a simple variable transformation to improve accuracy," in Proc. International Conference *From Galileo's "Occhialino" to Optoelectronics* (Ed. P. Mazzoldi), Singapore World Scientific, 916–921, 1993.
14. Taneja, A., and A. Sharma, "Propagation of beams through optical waveguiding structures: comparison of the beam propagation method (BPM) and the collocation method," *J. Opt. Soc. Am. A*, Vol. 10, 1739–1745, 1993.
15. Sharma, A., and S. Banerjee, "A numerical method for solving the generalized equation for nonlinear pulse propagation through optical fibers" in *Proc. Conference on Emerging Optoelectronic Technologies*, New Delhi Tata McGraw-Hill, 366–369, 1992.
16. Deb, S., and A. Sharma, "Nonlinear pulse propagation through optical fibers: an efficient numerical method," *Opt. Eng.*, Vol. 32, 695–699, 1993; Errata: Vol. 32, 2986, 1993.
17. Deb, S., A. Taneja, and A. Sharma, "Wave propagation through a randomly perturbed waveguide using the collocation method," (to be published).

18. Frazer, R. A., W. P. Jones, and S. W. Skan, "Approximations to functions and to the solution of differential equations," *Gt. Brit. Aero. Res. Council Rept. and Memo., 1799*; Reprinted in *Gt. Brit. Air Ministry Aero. Res. Comm. Tech. Rept.*, Vol. 1, 517–549, 1937.
19. Lanczos, C., "Trignometric interpolation of empirical and analytical functions," *J. Math. Phys.*, Vol. 17, 123–199, 1938.
20. Lanczos, C., *Applied Analysis*, Englewood Cliffs(NJ) Prentice, 1956.
21. Finlayson, B. A., and L. E. Scriven, "The method of weighted residuals – a review," *Appl. Mech. Rev.*, Vol. 19, 735–748, 1966.
22. Villadsen, J. V., and W. E. Stewart, "Solution of boundary value problems by orthogonal collocation," *Chem. Engg. Sci.*, Vol. 22, 1483–1501, 1967.
23. Fletcher, C. A. J., *Computational Galerkin Methods*, New York, Springer, 1984.
24. Finlayson, B. A., *Method of Weighted Residuals and Variational Principles with Applications to Fluid Mechanics, Heat and Mass Transfer*, New York Academic, 1972.
25. Abramowitz, M., and I. A. Stegun, *Handbook of Mathematical Functions*, New York Dover, 1964.
26. Stroud, A. H., and D. Secrest, *Gaussian Quadrature Formulas*, Englewood Cliffs (NJ) Prentice Hall, 1966.
27. Scarborough, J. B., *Numerical Mathematical Analysis*, London Oxford University Press, 1966.
28. Adams, M. J., *An Introduction to Optical Waveguides*, Chichester Wiley, 1981.
29. Yevick, D., and B. Hermansson, "New approach to perturbed optical waveguides," *Opt. Lett.*, Vol. 11, 103–105, 1986.
30. Gear, C. W., *Numerical Initial Value Problems in Ordinary Differential Equations,* Englewood Cliffs (NJ) Prentice-Hall, 1971.
31. Aitken, R. C., (ed.), *Stiff Computations*, New York Oxford Press, 1985.
32. Hall, G., and J. M. Watt, *Modern Numerical Methods for Ordinary Differential Equation*, Oxford Clarendon, 1976.
33. Rahman, B. M. A., and J. B. Davies, "Finite-element analysis of optical and microwave waveguide problems," *IEEE Trans. Microwave Theory Tech.*, Vol. MTT-32, 20–28, 1984.

34. Scarmozzino, R., and R. M. Osgood, Jr., "Comparison of finite-difference and Fourier-transform solutions of the parabolic wave equation with emphasis on integrated optic applications," *J. Opt. Soc. Am. A*, Vol. 8, 724–731, 1991.
35. Knox, R. M., and P. P. Toulis, "Integrated circuits for millimeter through optical frequency range," *Symp. Submillimeter Waves*, Broohlyn Polytechnic Institute, 1970.
36. Hocker, G. B., and W. K. Burns, "Mode dispersion in diffused channel waveguides by the effective index method," *Appl. Opt.*, Vol. 16, 113–118, 1977.
37. Sharma, A., "On approximate theories of single mode rectangular waveguides," *Opt. Quantum Electron.*, Vol. 21, 517–520, 1989.
38. Sharma, A., "A method for obtaining optimum equivalent 1-D index profiles for 2-D index profiles of optical waveguides," *Optics in Complex Systems*, F.Lanzl, H.-J. Preuss, G.Weigelt, eds., *Proc. SPIE*, Vol. 1319, 118, 1990.
39. Mevenkemp, W., and E. Voges, "Modeling and beam propagation analysis of integrated electro-optic devices," *A E Ü*, Vol. 40, 289–296, 1986.
40. Marcatili, E. A. J., and A. A. Hardy, "The azimuthal effective index method," *IEEE J. Quantum Electron.*, Vol. QE-24, 766–774, 1988.
41. Komori, K., S. Arai, Y. Suematsu, I. Arima, and M. Aoki, "Single mode properties of distributed reflector lasers," *IEEE J. Quantum Electron.*, Vol. QE-25, 1235–1244, 1989.
42. Wang, S., "Principles of distributed feedback and distributed Bragg reflector lasers," *IEEE J.Quantum Electron.*, Vol. QE-10, 413–427, 1974.
43. Hadjicostas, G., J. K. Butler, G. A. Evans, N. W. Carlson, and R. Amantea, "A numerical investigation of wave interactions in dielectric waveguides with periodic surface corrugations," *IEEE J. Quantum Electron.*, Vol. QE-26, 893–902, 1990.
44. Kogelnik, H., and C. V. Shank, "Coupled wave theory of distributed feedback lasers," *J. Appl. Phys.*, Vol. 43, 2327–2335, 1972.
45. Jaggard, D. L., and C. Elachi, "Floquet and coupled wave analysis of higher order Bragg coupling in a periodic medium," *J. Opt. Soc. Am.*, Vol. 66, 537–539, 1975.

46. Sharma, A., and S. Deb, "Wave propagation through peiodic waveguides: a numerical simulation method," Presented at *Linear and Nonlinear Integrated Optics Conference* in *International Symposium on Integrated Optics*, Lindau (Germany), April 11–15, 1994 (to appear in *Proc. SPIE*, Vol. 2212).
47. Ballman, R., *Introduction to Matrix Analysis*, New York McGraw Hill, 1960.
48. Agrawal, G. P., and A. H. Bobeck, "Modeling of distributed feedback semiconductor lasers with axially-varying parameters," *IEEE J. Quantum Electron.*, Vol. QE-24, 2407–2414, 1988.
49. Haus, H. A., *Waves and Fields in Optoelectronics*, Englewood Cliffs Prentice-Hall, 1984.
50. Uscinski, B. J., *Elements of Wave Propagation in Random Media*, London McGraw-Hill, 1977.
51. Tatarskii, V. I., *The Effects of the Turbulent Atmosphere on Wave Propagation*, Springfield National Technical Information Service, 1971.
52. Ishimaru, A., *Wave Propagation and Scattering in Random Media*, New York Academic, 1978.
53. Prokhorov, A. M., F. V. Bunkin, K. S. Gochelashvily, and V. I. Shishov, "Laser irradiance propagation in turbulent media," *Proc. IEEE*, Vol. 63, 790–811, 1975.
54. Fante, R. L., "Electromagnetic beam propagation in turbulent media: an update," *Proc. IEEE*, Vol. 68, 1424–1444, 1980.
55. Brown, W. P.,Jr., "Fourth moment of a wave propagating in a random medium," *J. Opt. Soc. Am.*, Vol. 62, 966–971, 1972.
56. Tur, M., and M. J. Beran, "Propagation of a finite beam through a random medium," *Opt. Lett.*, Vol. 5, 306–308, 1982.
57. Gozani J., "Numerical solution for the fourth order coherence function of a plane wave propagating in a two-dimensional Kolmogorovian medium," *J. Opt. Soc. Am. A*, Vol. 2, 2144–2151, 1985.
58. Flatte, S. M., and F. D. Tappert, "Calculation of the effect of internal waves on oceanic sound transmission," *J. Acoust. Soc. Am.*, Vol. 58, 1151–1159, 1975.
59. Goyal, I. C., M. S. Sodha, and A. K. Ghatak, "Propagation of electromagnetic waves in a medium with random radial dielectric-constant gradient," *J. Opt. Soc. Am.*, Vol. 63, 940–943, 1973.

60. Sharma, A., I. C. Goyal, N. K. Bansal, and A. K. Ghatak, "Propagation of gaussian beams through parabolic-index optical waveguides with random dielectric constant gradient," *Fiber Integrated Optics*, Vol. 2, 299–314, 1979.
61. Papanicolaou, G. C., D. McLaughlin, and R. Burridge, "A stochastic gaussian beam," *J. Math. Phys.*, Vol. 14, 84–87, 1973.
62. Crosignani B., B. Daino, and P. D. Porto, "Statistical coupled equations in lossless optical fibers," *IEEE Trans. Microwave Theory Tech.*, Vol. MTT–23, 416–420, 1975.
63. Hasegawa, A., and F. Tappert, "Transmission of stationary nonlinear optical pulses in dispersive dielectric fibers, 1. Anomalous dispersion," *Appl. Phys.Lett.*, Vol. 142, 142–144, 1973.
64. Mollenauer, L. F., R. H. Stolen, and J. P. Gordon, "Experimental observation of picosecond pulse narrowing and solitons in optical fibers," *Phys. Rev. Lett.*, Vol. 45, 1095–1098, 1980.
65. Agrawal, G. P., *Nonlinear Fiber Optics*, Boston Academic, 1989.
66. Kumar, A., "Soliton dynamics in a monomode optical fiber," *Physics Reports*, Vol. 187, 63–108, 1990.
67. Satsuma, J., and N. Yajima, "Initial value problems of one dimensional self-modulation of nonlinear waves in dispersive media," *Prog. Theor. Phys. Suppl.*, Vol. 55, 284–306, 1973.
68. Schubert, M., and B. Wilhelmi, *Nonlinear Optics and Quantum Electronics*, New York John Wiley, 1986.
69. Fisher, R. A., and W. K. Bischel, "The role of linear dispersion in plane-wave self phase modulation," *Appl. Phys. Lett.*, Vol. 23, 661–663, 1973.
70. Hermansson, B., and D. Yevick, "Generalized propagation techniques – application to semiconductor rib waveguide Y-junctions," *Photon. Technol. Lett.*, Vol. 2, 738–740, 1990.
71. Glasner, M., D. Yevick, and B. Hermansson, "High-order generalized propagation techniques," *J. Opt. Soc. Am. B*, Vol. 8, 413–415, 1991
72. Hermansson, B., and D. Yevick, "Generalized propagation techniques," *Opt. Lett.*, Vol. 16, 354–356, 1991.